Design of Drilled Shafts in Iowa – Validation and Design Recommendations

Final Report
September 2024

IOWA STATE UNIVERSITY
Institute for Transportation

Sponsored by
Iowa Highway Research Board
(IHRB Project TR-763)
Iowa Department of Transportation
(InTrans Project 19-684)
Federal Highway Administration

About the Bridge Engineering Center

The mission of the Bridge Engineering Center (BEC) is to conduct research on bridge technologies to help bridge designers/owners design, build, and maintain long-lasting bridges.

About the Institute for Transportation

The mission of the Institute for Transportation (InTrans) at Iowa State University is to save lives and improve economic vitality through discovery, research innovation, outreach, and the implementation of bold ideas.

Iowa State University Nondiscrimination Statement

Iowa State University does not discriminate on the basis of race, color, age, ethnicity, religion, national origin, pregnancy, sexual orientation, gender identity, genetic information, sex, marital status, disability, or status as a US veteran. Inquiries regarding nondiscrimination policies may be directed to the Office of Equal Opportunity, 3410 Beardshear Hall, 515 Morrill Road, Ames, Iowa 50011, telephone: 515-294-7612, hotline: 515-294-1222, email: eooffice@iastate.edu.

Disclaimer Notice

The contents of this report reflect the views of the authors, who are responsible for the facts and the accuracy of the information presented herein. The opinions, findings and conclusions expressed in this publication are those of the authors and not necessarily those of the sponsors.

The sponsors assume no liability for the contents or use of the information contained in this document. This report does not constitute a standard, specification, or regulation.

The sponsors do not endorse products or manufacturers. Trademarks or manufacturers' names appear in this report only because they are considered essential to the objective of the document.

Quality Assurance Statement

The Federal Highway Administration (FHWA) provides high-quality information to serve Government, industry, and the public in a manner that promotes public understanding. Standards and policies are used to ensure and maximize the quality, objectivity, utility, and integrity of its information. The FHWA periodically reviews quality issues and adjusts its programs and processes to ensure continuous quality improvement.

Iowa DOT Statements

Federal and state laws prohibit employment and/or public accommodation discrimination on the basis of age, color, creed, disability, gender identity, national origin, pregnancy, race, religion, sex, sexual orientation or veteran's status. If you believe you have been discriminated against, please contact the Iowa Civil Rights Commission at 800-457-4416 or the Iowa Department of Transportation affirmative action officer. If you need accommodations because of a disability to access the Iowa Department of Transportation's services, contact the agency's affirmative action officer at 800-262-0003.

The preparation of this report was financed in part through funds provided by the Iowa Department of Transportation through its "Second Revised Agreement for the Management of Research Conducted by Iowa State University for the Iowa Department of Transportation" and its amendments.

The opinions, findings, and conclusions expressed in this publication are those of the authors and not necessarily those of the Iowa Department of Transportation or the U.S. Department of Transportation Federal Highway Administration.

Technical Report Documentation Page

1. Report No.	2. Government Accession No.	3. Recipient's Catalog No.
IHRB Project TR-763		

4. Title and Subtitle	5. Report Date
Design of Drilled Shafts in Iowa – Validation and Design Recommendations	September 2024
	6. Performing Organization Code
7. Author(s)	**8. Performing Organization Report No.**
Philippe Kalmogo (orcid.org/0000-0002-9727-5945), Rupsa Roy (orcid.org/0009-0006-8095-8009), Sri Sritharan (orcid.org/0000-0001-9941-8156), and Jeramy C. Ashlock (orcid.org/0000-0003-0677-9900)	InTrans Project 19-684
9. Performing Organization Name and Address	**10. Work Unit No. (TRAIS)**
Bridge Engineering Center Iowa State University 2711 South Loop Drive, Suite 4700 Ames, IA 50010-8664	**11. Contract or Grant No.**
12. Sponsoring Organization Name and Address	**13. Type of Report and Period Covered**
Iowa Department of Transportation 800 Lincoln Way Ames, IA 50010 Federal Highway Administration U.S. Department of Transportation 1200 New Jersey Avenue SE Washington, DC 20590	Final Report
	14. Sponsoring Agency Code

15. Supplementary Notes

Visit https://intrans.iastate.edu for color PDFs of this and other research reports.

16. Abstract

The design of drilled shafts in Iowa currently relies on the American Association of State Highway and Transportation Officials (AASHTO) *LRFD Bridge Design Specifications*. To improve design efficiency at the state level, a series of research projects was conducted to develop the Drilled SHAft Foundation Testing (DSHAFT) database, a regional database facilitating the collection, storage, and efficient access of load test data from Iowa and other states, and to utilize the collected data to establish regional resistance factors that are reflective of the uncertainties associated with predicting drilled shaft capacity under Iowa's specific geological conditions and construction practices. Resistance factors established in a 2019 study for various resistance prediction methods generally showed improvements over those recommended by AASHTO.

The present research aimed to validate the proposed resistance factors and formulate design recommendations for implementation. To this end, the DSHAFT database was further expanded with additional test data. Additionally, regression analyses were conducted on test data from Iowa to develop local resistance predictions that may provide more accurate estimates of drilled shaft capacity locally. Results from the analysis indicated that a linear correlation between soil parameters and measured unit side resistance was the best fit for most soil types. Moreover, settlement data were collected at several production shafts that were part of a few Iowa DOT bridge replacement projects to evaluate the field performance of drilled shafts designed under the current Iowa DOT guidelines. Various challenges were encountered during the data collection process. Some of the data indicated unexpected negative settlements, and further investigation is needed to develop appropriate conclusions. Design recommendations were formulated based on all findings, and design examples were developed to illustrate the application of the design recommendations.

17. Key Words	18. Distribution Statement
bridge design—drilled shafts—settlement—resistance factors—side resistance—LRFD	No restrictions.

19. Security Classification (of this report)	20. Security Classification (of this page)	21. No. of Pages	22. Price
Unclassified.	Unclassified.	85	NA

Form DOT F 1700.7 (8-72) **Reproduction of completed page authorized**

DESIGN OF DRILLED SHAFTS IN IOWA – VALIDATION AND DESIGN RECOMMENDATIONS

Draft Report
September 2024

Principal Investigator
Sri Sritharan, Wilkinson Chair Professor of Interdisciplinary Engineering
Department of Civil, Construction, and Environmental Engineering, Iowa State University

Co-Principal Investigator
Jeramy C. Ashlock, Associate Professor
Department of Civil, Construction, and Environmental Engineering, Iowa State University

Research Assistants
Philippe Kalmogo and Rupsa Roy

Sponsored by
Iowa Highway Research Board and
Iowa Department of Transportation
(IHRB Project TR-763)

Preparation of this report was financed in part
through funds provided by the Iowa Department of Transportation
through its Research Management Agreement with the
Institute for Transportation
(InTrans Project 19-684)

A report from
Bridge Engineering Center
Iowa State University
2711 South Loop Drive, Suite 4700
Ames, IA 50010-8664
Phone: 515-294-8103 Fax: 515-294-0467
https://bec.iastate.edu

TABLE OF CONTENTS

LIST OF FIGURES

LIST OF TABLES

ACKNOWLEDGMENTS

The research team would like to thank the Iowa Department of Transportation (DOT) and Iowa Highway Research Board (IHRB) for sponsoring this research and the technical advisory committee (TAC) for their guidance.

EXECUTIVE SUMMARY

The design of drilled shafts in Iowa currently relies on the American Association of State Highway and Transportation Officials (AASHTO) *LRFD Bridge Design Specifications*. To improve design efficiency at the state level, a series of research projects was conducted to develop the Drilled SHAft Foundation Testing (DSHAFT) database, a regional database facilitating the collection, storage, and efficient access of load test data from Iowa and other states, and to utilize the collected data to establish regional resistance factors that are reflective of the uncertainties associated with predicting drilled shaft capacity under Iowa's specific geological conditions and construction practices. Resistance factors established by Kalmogo et al. (2019) for various resistance prediction methods generally showed improvements over those recommended by AASHTO (2017).

The present research aimed to validate the proposed resistance factors and formulate design recommendations for implementation. To this end, the DSHAFT database was further expanded with additional test data. Additionally, regression analyses were conducted on test data from Iowa to develop local resistance predictions that may provide more accurate estimates of drilled shaft capacity locally. Results from the analysis indicated that a linear correlation between soil parameters and measured unit side resistance was the best fit for most soil types. Moreover, settlement data were collected at several production shafts that were part of a few Iowa DOT bridge replacement projects to evaluate the field performance of drilled shafts designed under the current Iowa DOT guidelines. Various challenges were encountered during the data collection process. Some of the data indicated unexpected negative settlements, and further investigation is needed to develop appropriate conclusions. Design recommendations were formulated based on all findings, and design examples were developed to illustrate the application of the design recommendations.

CHAPTER 1. OVERVIEW

1.1. Background

The use of drilled shafts to support highway bridges in the state of Iowa has significantly increased in recent years. Drilled shafts are more efficient and cost-effective than the commonly used driven piles for certain ground and construction site conditions. Current design guidelines in the Iowa *Bridge Design Manual* (2024) for the load and resistance factor design (LRFD) and construction of drilled shafts rely primarily on Brown et al. (2018) and the American Association of State Highway and Transportation Officials (AASHTO) *LRFD Bridge Design Specifications* (AASHTO 2017). Although these specifications have allowed the Iowa Department of Transportation (DOT) Bridges and Structures Bureau to design all bridges in accordance with the Federal Highway Administration (FHWA) mandate to use the LRFD approach on all federally funded bridges initiated after October 1, 2007, the recommended resistance factors for drilled shaft design, specifically for axial loading, have several limitations. These factors were developed primarily by fitting to previously used allowable strength design (ASD) factors of safety (Brown et al. 2018), and they were evaluated against the resistance factors calculated by Allen (2005) using probability-based reliability methods based on a general national database before final values were adopted. The recommended factors were not specifically developed for the state of Iowa, and therefore they may not accurately reflect local geological conditions and construction practices. Local geological conditions and construction techniques significantly affect the accuracy of estimates of drilled shafts' field performance. As such, it is of paramount importance to establish resistance factors at regional levels utilizing a local high-quality load test database.

To this end, a series of research projects funded by the Iowa DOT was conducted that led to the development of a regional Database for Drilled SHAft Foundation Testing (DSHAFT) and the calibration of regional resistance factors based on the data included in the database (Garder et al. 2012, Ng et al. 2014, Kalmogo et al. 2019). Resistance factors were developed for various resistance prediction methods for cohesive soils, cohesionless soils, cohesive intermediate geomaterials (IGM), and rock. Resistance factors proposed by Kalmogo et al. (2019) were developed with no extrapolation of non-failed tests using layered and global approaches. In the layered approach, shear zones of the same geomaterial type in a given test shaft were treated independently, and the resistance bias was calculated as the ratio of the measured to predicted resistance for each individual shear zone. In the global approach, the resistance bias was calculated as the sum of the measured to predicted resistances from shear zones of the same geomaterial category. Generally, the global approach produced higher resistance factors than the local approach due to a higher level of error in estimating the resistance of individual shear zones or soil layers. Overall, the calibrated factors using the global approach showed improvement over AASHTO's recommended factors except for resistance prediction in cohesive soils and rock using O'Neill and Reese (1999) and Kulhawy et al. (2005), respectively.

1.2. Scope of Research Project

The overall goal of this project was to provide final recommendations for the design and construction of drilled shafts in Iowa in accordance with the LRFD framework using additional load test data. This was accomplished by (1) expanding the DSHAFT database, (2) conducting regression analyses on the data to develop local design methods, (3) monitoring and analyzing settlement of production shafts, (4) formulating design recommendations, and (5) developing design examples to illustrate applications of the design recommendations.

1.3. Report Organization

The purpose of this report is to illustrate the validation of previously calibrated resistance factors and recommendations for the LRFD of drilled shafts under axial loads in Iowa. This report consists of six chapters. The content of each chapter is briefly described as follows:

- **Chapter 1. Overview**. A brief description of the background of resistance factor calibration for drilled shafts in Iowa and the scope of the research project.
- **Chapter 2. DSHAFT Database Expansion**. A description of additional load test data collected from Iowa, Nebraska, and Illinois that were analyzed and included in DSHAFT.
- **Chapter 3. Load Test Data Analysis.** A description of the regression analyses conducted on the load test data available in DSHAFT. Correlations were determined between soil parameters and measured unit side resistance.
- **Chapter 4. Monitoring and Analysis of the Settlement of Production Shafts.** A description of the instrumentation of production shafts in Iowa DOT bridge replacement projects and the measurement and analysis of settlement.
- **Chapter 5. Design Recommendations.** A description of design recommendations for drilled shafts in Iowa based on the findings of this project.
- **Chapter 6. Summary and Future Work.** A summary of the research outcomes for the development of regional LRFD procedures for drilled shafts in Iowa and proposed topics for future research.
- **Appendix. Design Examples**. A description of design examples illustrating the design recommendations presented in Chapter 5.

CHAPTER 2. DSHAFT DATABASE EXPANSION

The DSHAFT database was developed with the primary objective of enabling the efficient collection, access, and analysis of drilled shaft field load test data. Such data are required for the statistical characterization of the uncertainties involved in the calculation of drilled shaft side and tip resistances and for the calibration of resistance factors for design within the LRFD framework. The database was developed in the initial phase of this project by Garder et al. (2012) and was later expanded with additional test data by Ng et al. (2014) and Kalmogo et al. (2019). As more load tests are performed that provide additional data on drilled shaft field performance, it is essential that the database be updated to improve its quality and enable a refinement of previously calibrated resistance factors through an improved statistical characterization of resistance uncertainties. In addition to the calibration of resistance factors, statistical analyses can be performed on the data to investigate correlations between measured resistances and soil parameters and thus develop state-specific resistance calculation methods that are more efficient than those recommended by existing design manuals and national codes.

As such, one of the tasks of this project was to gather new load test data through a review of the literature or direct requests to the Minnesota, Iowa, Illinois, Nebraska, and Wisconsin DOTs. Of these agencies, data were obtained from Iowa, Illinois, and Nebraska. All load test data were obtained from bi-directional tests conducted on instrumented drilled shafts following ASTM D8169-18 Procedure A, Quick Test, in soil profiles that included various types of geomaterials.

2.1. Nebraska

Two Osterberg cell (O-cell) load tests were conducted as part of a major lane expansion project led by the Nebraska DOT on an 18.5-mile segment of the US 275 expressway located between Scribner and West Point. The first shaft, TS1, included a 52.3 ft long segment above the O-cell and a 37.6 ft segment below the O-cell. The nominal diameter of the shaft was 67 in. along the upper 8 ft as a result of the permanent casing used during construction. Below the tip of the casing, the nominal shaft diameter was 60 in. As observed in the boring performed, the soil profile at TS1 consisted of 13 ft of fat clay, 7 ft of lean clay, 16.5 ft of sand with silt, 2.5 ft of lean clay, 7.5 ft of silty sand, 70.5 ft of fat clay, and 26.5 ft of sand with silt. The water table was located at an elevation of +1,256.1 ft, 12.3 ft below the existing ground surface. The shaft was excavated under bentonite slurry to a base elevation of +1,173 ft. After cleaning out the shaft base and profiling the excavation, the reinforcing cage was installed, and concrete was poured from the base to a shaft top elevation of +1,263 ft.

The second shaft, TS2, was composed of an 85.7 ft long segment above the O-cell and a 36 ft segment below the O-cell. A temporary casing was used during construction, resulting in a nominal shaft diameter of 72 in. in the upper 15 ft of the shaft. The nominal diameter in the remainder of the shaft was 66 in. The boring performed at the shaft location indicated a soil profile consisting of 6 ft of lean clay, 1.5 ft of silty clay, 5 ft of sand, 31.5 ft of sand with silt, and 81 ft of fat clay. The water table was located at an elevation of +1,260 ft, 6.6 ft below the existing ground surface. The shaft was excavated under bentonite slurry to a base elevation of +1,137 ft. After cleaning out the shaft base and profiling the excavation, the reinforcing cage was installed, and concrete was poured from the base to a shaft top elevation of +1,258.7 ft.

Each of the shafts was instrumented with three levels of two vibrating wire strain gauges for strain measurements and telltales to measure the shaft displacement and compression. Linear vibrating wire strain displacement transducers (LVWDTs) were also installed between the upper and lower plates of the O-cell assembly to measure their displacements.

For TS1, maximum net loads of 499 kips and 614 kips were applied to the upper and lower segments, respectively, over 25 load increments. The corresponding displacements at these loads were 0.33 in. and 0.10 in. for the upper and lower segments, respectively. TS2 was loaded to maximum applied net loads of 1,382 kips and 1,581 kips for the upper and lower shaft segments, respectively, over 20 load increments. The corresponding displacements were 0.37 in. for the upper segment and 0.41 in. for the lower segment. It is worth noting that both shafts were planned to be used as production shafts after the tests, and therefore the maximum loads applied during the tests were likely less than the magnitude that would be required to achieve the ultimate condition. Data obtained from the strain gauges were analyzed to establish the load distribution along each shaft at each load increment performed during the test. The load distribution curves were subsequently utilized to calculate the average unit side shear in the soil within any two levels of strain gauges as well as the unit tip resistance at the base of the shaft. The unit side shear values calculated at the last load increment are shown in Table 1 and Table 2 for TS1 and TS2, respectively.

Table 1. Average net side shear for TS1

Load Transfer Zone	Net Unit Side Shear (ksf)
Zero Shear to Strain Gauge 3	0.5
Strain Gage Level 3 to Strain Gage Level 2	0.5
Strain Gage Level 2 to O-cell	0.7
O-cell to Strain Gage Level 1	0.9

Table 2. Average net side shear for TS2

Load Transfer Zone	Net Unit Side Shear (ksf)
Zero Shear to Strain Gauge 3	0.5
Strain Gage Level 3 to O-cell	1.1
O-cell to Strain Gage Level 2	1.0
Strain Gage Level 2 to Strain Gage Level 1	1.7

For TS1, a maximum unit end bearing of 5.1 ksf was calculated assuming a unit side shear of 0.9 ksf for the short shaft segment located between Strain Gage Level 1 and the base of the shaft. The corresponding displacement at this end bearing was determined to be 0.088 in. For TS2, the maximum unit end bearing was found to be 22.8 ksf at a corresponding base displacement of 0.34 in. Additional details on the soil profile at the shaft location and on the construction, instrumentation, and testing of the shaft can be found in the load test reports provided in the DSHAFT database.

2.2. Illinois

Test data obtained from the state of Illinois included two O-cell load tests that were conducted at two bridge sites, including IL 89 over the Illinois River near Spring Valley, Illinois, and IL 133 over the Embarras River near Oakland, Illinois.

2.2.1. Bridge Site at IL 89 over the Illinois River

The subsurface condition at the test shaft location for this site was established based on four borings performed near the shaft. As shown in Figure 1, the subsurface profile included overburden soils consisting of 10 ft of silty loam; 25 ft of brown, stiff, silty clay; 7 ft of medium-dense sand; and 17.5 ft of brown, stiff, silty clay. The overburden soils were underlain by a thinly bedded clay-shale formation. The unconfined compression strength of the cohesive soils in the profile was determined from unconfined compression tests on rock core samples and from modified standard penetration test (MSPT) penetration rate data.

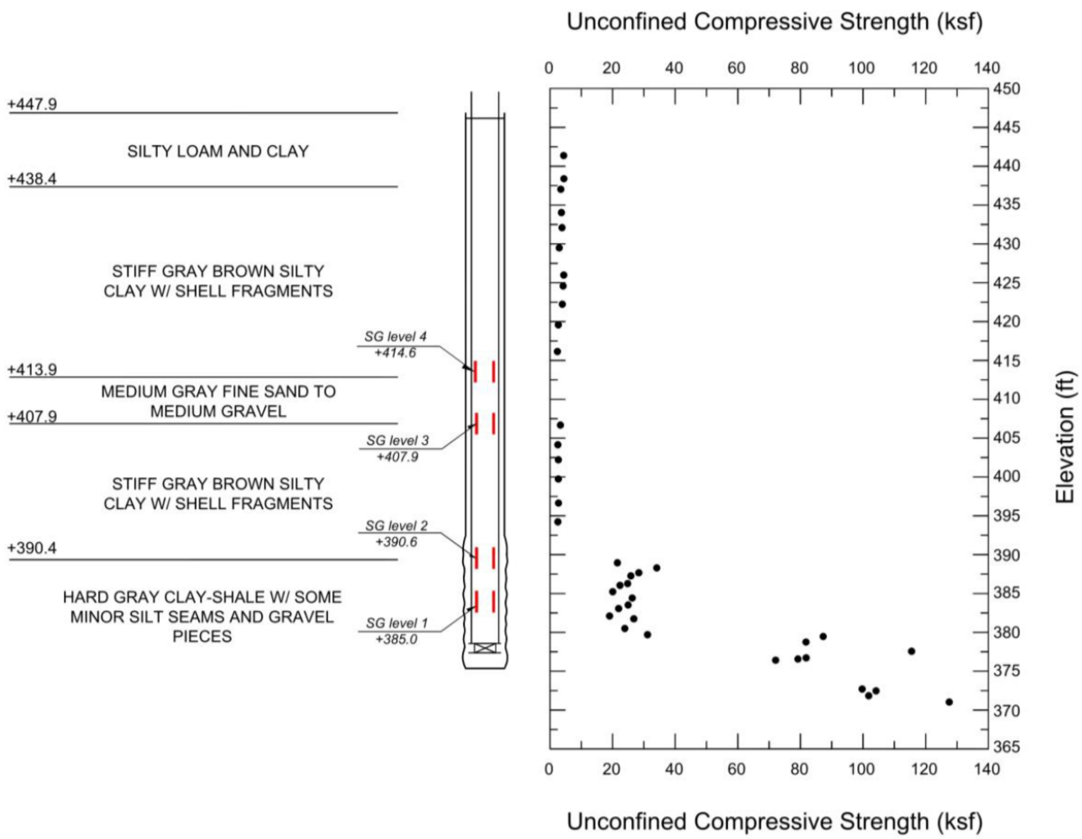

Stark et al. 2017

Figure 1. Idealized subsurface profile and test shaft schematic for the bridge site at IL 89 over the Illinois River

The shaft had a nominal diameter of 60 in. and was embedded 70.8 ft below the existing ground surface. A permanent casing was used in the portion of the shaft within the overburden soils during construction, as described by Stark et al. (2017). The O-cell was located 2 ft above the tip of the shaft. The instrumentation plan for the shaft included four levels of two vibrating wire strain gauges as well as compression telltales and LVWDTs. Cross-hole sonic logging (CSL) tubes with diameters of 2 in. were also included along the full length of the shaft to perform integrity testing of the concrete after installation.

As shown in Figure 2, a maximum sustained bi-directional load of 1,551 kips was applied to the shaft, inducing 0.355 in. and 0.158 in. of displacement above and below the O-cell, respectively. Failure of the shaft segment above the O-cell occurred beyond this magnitude of loading. At the ultimate stage, the maximum bi-directional load was 1,713 kips, and the recorded maximum displacements were 1.66 and 0.19 in. above and below the O-cell, respectively. Load distribution curves at all load increments were established based on the strain gauge data and were used to determine the load transfer curves along the side (t-z) and at the base (q-z) of the shaft, which are shown in Figure 3 and Figure 4, respectively. The average unit side shear values calculated at the maximum sustained load are shown in Table 3. A maximum unit end bearing of 66.8 ksf was recorded at a corresponding base displacement of 0.19 in.

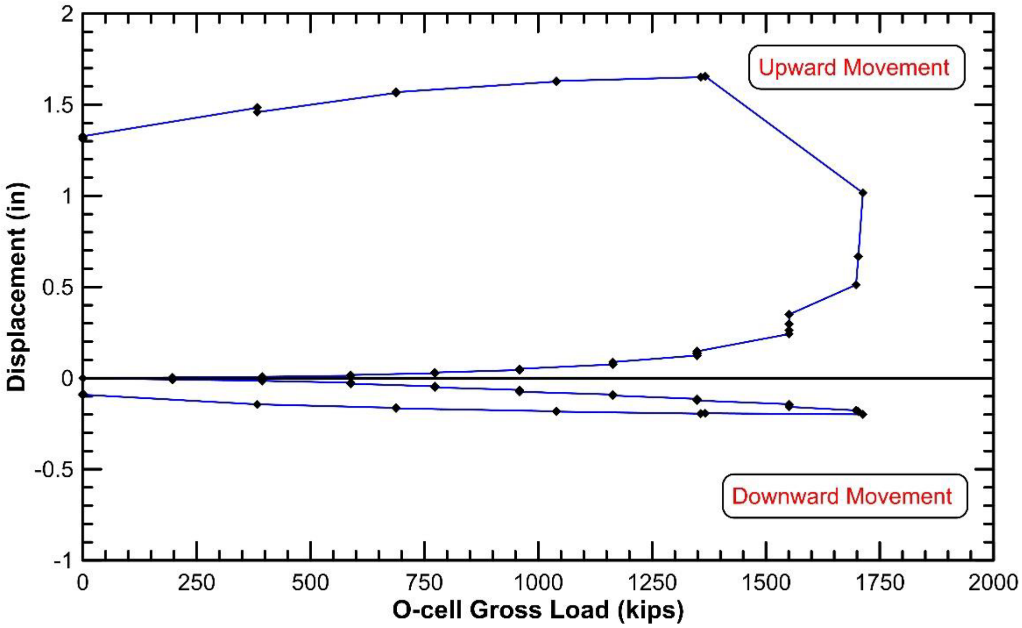

Stark et al. 2017

Figure 2. Load-displacement curves of the shaft above and below the O-cell for the load test at IL 89 over the Illinois River

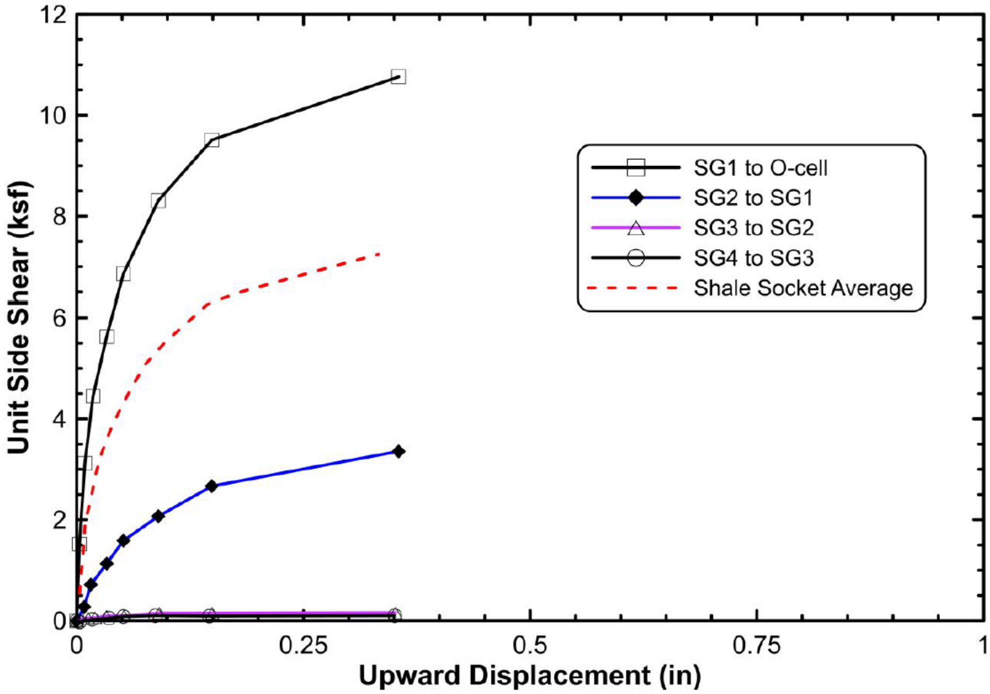

Stark et al. 2017

Figure 3. Mobilized unit side resistance for the test shaft at IL 89 over the Illinois River

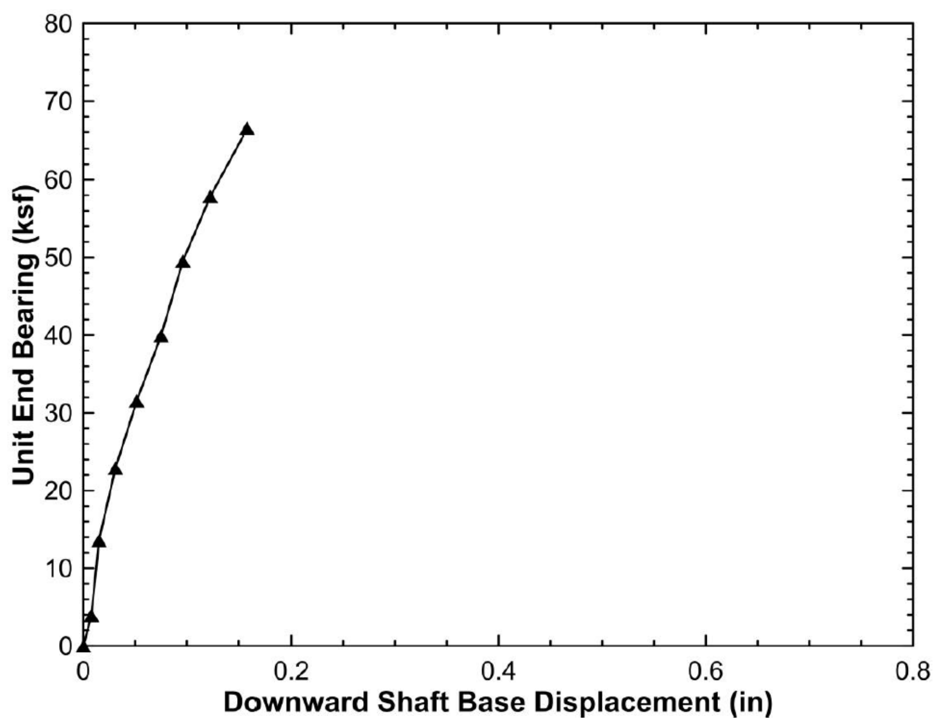

Stark et al. 2017

Figure 4. Mobilized unit tip resistance for the test shaft at IL 89 over the Illinois River

Table 3. Average unit side shear for the bridge site at IL 89 over the Illinois River

Load Transfer Zone	Net Unit Side Shear (ksf)
Strain Gauge 4 to Strain Gauge 3	0.2
Strain Gage Level 3 to Strain Gage Level 2	0.1
Strain Gage Level 2 to Strain Gage Level 1	3.3
Strain Gage Level 1 to O-cell	10.7

2.2.2. Bridge Site at IL 133 over the Embarras River

Subsurface conditions at the bridge site at IL 133 over the Embarras River were established based on four borings using testing methods similar to those used at the bridge site at IL 89 over the Illinois River. As shown in Figure 5, the idealized soil profile consisted of weathered clay shale bedrock overlain by about 11 ft of soft to stiff silty clay. The test shaft had a nominal diameter of 48 in. and a length of 24.3 ft. The shaft was excavated under dry conditions with a 54 in. diameter temporary casing providing support within the overburden soil. The O-cell in this test was located about 2.3 ft above the shaft base. Instrumentation consisted of three levels of four vibrating wire gauges as well as compression telltales and LVWDTs, similar to the instrumentation used for the test shaft at the bridge site at IL 89 over the Illinois River. The integrity of the shaft was evaluated using the CSL tubes installed in the shaft.

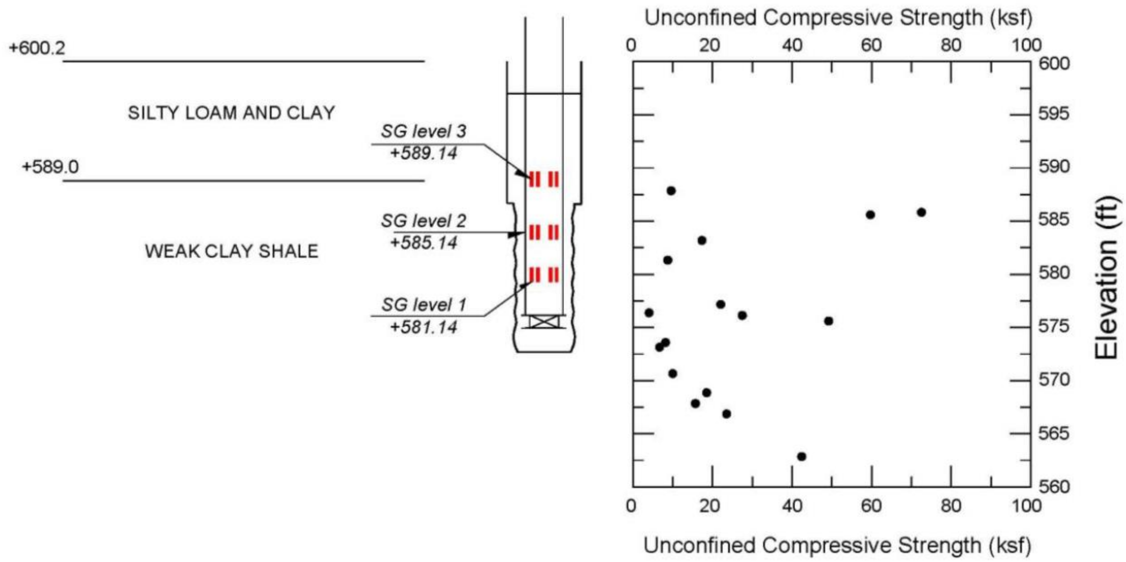

Stark et al. 2017

Figure 5. Idealized subsurface profile and test shaft schematic for the bridge site at IL 133 over the Embarras River

The shaft was loaded to a maximum sustained loading of 913 kips with corresponding displacements of 1.282 and 1.684 in. above and below the O-cell, respectively. Failure of the shaft segment above the O-cell occurred when the load was increased to 993 kips, resulting in displacements of 4.155 and 1.929 in. above and below the O-cell, respectively. The calculated average unit side shear at the maximum sustained loading are shown in Table 4. The maximum unit end bearing was calculated to be about 58 ksf at a shaft base displacement of 1.64 in.

Table 4. Average unit side shear for the bridge site at IL 133 over the Embarras River

Load Transfer Zone	Net Unit Side Shear (ksf)
Strain Gage Level 3 to Strain Gage Level 2	2.4
Strain Gage Level 2 to Strain Gage Level 1	7.4
Strain Gage Level 1 to O-cell	6.3

2.3. Iowa

2.3.1. Bridge Site at I-74 over Mississippi River

The mudline at the I-74 bridge over the Mississippi River was located at an elevation of +545 ft, about 15 ft below the water surface. Below the mudline, the soil profile consisted of 6.5 ft of gravel, 4.5 ft of silty sand, and 10 ft of slightly weathered sandstone overlying a moderately weathered limestone bedrock. The test shaft was excavated under water to a base elevation of +521.8 ft with the support of a permanent casing installed through the overburden soil to an elevation of +536.3 ft. After cleaning out the base and installing the reinforcing cage, concrete was poured from the base to a top elevation of +559.5 ft. Due to an issue with concrete supply, the concrete for the entire shaft was poured in two stages instead of in the typical one stage. The nominal diameter of the shaft was 84 in. within the permanent casing and 78 in. between the bottom of the casing and the shaft base. The O-cell was located at an elevation of +522.2 ft. The shaft was instrumented with one level of four vibrating wire strain gauges and one level of two gauges, compression telltales, and LVWDTs.

During the test, the shaft was loaded to a maximum sustained bi-directional load of 2,642 kips over 11 increments. The twelfth load increment, corresponding to a load of 2,829 kips, could not be sustained because the shaft segment above the O-cell reached its ultimate side shear capacity. At this loading, the displacements above and below the O-cell were 1.32 in. and 0.46 in., respectively. Average unit side shear values calculated at the maximum sustained loading are shown in Table 5. A maximum mobilized end bearing resistance of 181 ksf was calculated for a corresponding base displacement of 0.44 in.

Table 5. Average unit side shear for the bridge site at I-74 over the Mississippi River

Load Transfer Zone	Net Unit Side Shear (ksf)
Zero Shear to Strain Gage Level 2	0.5
Strain Gage Level 2 to Strain Gage Level 1	3.3
Strain Gage Level 1 to O-cell	15.3

2.3.2. US 52/IA 64 Bridge over the Mississippi River

At the bridge site at US 52/IA 64 over the Mississippi River, the mudline was located at an elevation of +567 ft, 13.5 ft below the water surface. Below the mudline, the soil profile included 4 ft of silty clay and 135 ft of sand overlying a limestone bedrock.

The test shaft was excavated under polymer slurry to a base elevation of +435.5 ft with the support of temporary and permanent casings installed to elevations of +553 ft and +530 ft, respectively. After the base of the shaft was cleaned and profiling of the excavation using the SONICaliper was complete, the reinforcing cage was installed, and concrete was poured from the base to a top elevation of +553 ft. The nominal diameter of the shaft was 79 in. within the permanent casing and 72 in. between the bottom of the casing and the shaft base. The O-cell was located at an elevation of +454.5 ft, 19 ft above the base of the shaft. The shaft was instrumented with nine levels of four vibrating wire strain gauges, compression telltales, and LVWDTs.

During the test, the shaft was loaded to a maximum sustained bi-directional load of 1,855 kips over eight equal increments. The ninth load increment could not be sustained due to side shear failure of the upper shaft segment. At the maximum applied load of 1,890 kips, the displacements above and below the O-cell were 1.05 in. and 0.73 in., respectively. Average unit side shear values calculated at the maximum sustained loading are shown in Table 5. A maximum mobilized end bearing resistance of 181 ksf was calculated for a corresponding base displacement of 0.44 in. The maximum mobilized end bearing resistance was 45.2 ksf for a corresponding base displacement of 0.71 in.

Table 6. Average unit side shear for the bridge site at US 52/IA 64 over the Mississippi River

Load Transfer Zone	Net Unit Side Shear (ksf)
Zero Shear to Strain Gage Level 9	0.0
Strain Gage Level 9 to Strain Gage Level 8	0.3
Strain Gage Level 8 to Strain Gage Level 7	0.5
Strain Gage Level 7 to Strain Gage Level 6	1.0
Strain Gage Level 6 to Strain Gage Level 5	0.9
Strain Gage Level 5 to Strain Gage Level 4	1.0
Strain Gage Level 4 to Strain Gage Level 3	1.3
Strain Gage Level 3 to O-cell	2.2
O-cell to Strain Gage 2	2.5
Strain Gage Level 2 to Strain Gage Level 1	1.2

CHAPTER 3. LOAD TEST DATA ANALYSIS

Various methods to estimate the side and end bearing resistance of axially loaded drilled shafts exist in the literature. Some have been adopted by the *AASHTO LRFD Bridge Design Specifications* (AASHTO 2017) and are used for routine design by multiple state agencies. Several of these methods are empirical or semi-empirical and have been developed using load test data from a wide range of locations with varying geologies that may not always be applicable to any specific region. As such, resistance prediction using these methods may be highly variable, resulting in the necessity of using relatively low resistance factors that can lead to costly designs.

The accuracy of drilled shaft capacity predictions can be improved through the development and implementation of local design methods based on load test data specific to a given region. Therefore, the measured resistance data obtained from tests performed in Iowa and included in the DSHAFT database were analyzed to investigate the correlation between measured resistance and soil parameters and to propose alternative design methods. The tests considered were conducted on instrumented drilled shafts with strain gauges installed at multiple locations along the length of each shaft. Strain data collected during testing were utilized to develop load distribution curves for each load increment. Then, the load distribution curves were used to establish the unit side and end bearing resistance as a function of shaft displacement for the geomaterial type found within any given pair of strain gauge levels. Several load tests were concluded before the geotechnical capacity of the shafts was reached because shaft capacity was underestimated during the planning phase of these tests and an O-cell with insufficient capacity was used.

For the analyses, a layered approach was utilized to categorize the test data into cohesive soil, cohesionless soil, cohesive IGM, and rock as defined by Brown et al. (2018). Measured geomaterial parameters in the database were limited to standard penetration test (SPT) blow counts (N) for soils and to unconfined compressive strength (UCS) and rock quality designation (RQD) for cohesive IGM and rock.

When developing correlations, it is essential that a failure criterion be selected to define geotechnical capacity. Capacity could be defined in terms of shaft displacement or in terms of plunging failure when the shaft can no longer sustain additional loading without very large displacements. A displacement-based criterion is generally more suitable than other criteria to define the geotechnical capacity of drilled shafts. Initially, a shaft top displacement of 1 in. was selected for the analyses herein, as consistent with Iowa DOT practice. However, the quantity of measured resistance data available at this criterion was low and led to sample sizes that were not statistically significant to investigate correlations between shaft resistance and known soil parameters. Therefore, the selected criterion to define capacity could not be used. Instead, the maximum measured resistance was selected regardless of the displacement achieved by the shaft, although this approach introduces a higher-than-desirable level of variability in the analyses. The alternative approach of extrapolating the data to the target displacement was not used given the potential of overestimating the actual shaft resistance.

Regression analyses were conducted on the data sets. The functions considered included linear, polynomial, exponential, power, and logarithmic.

3.1. Cohesive Soils

The cohesive soil category included 18 data points from 11 load tests representing unit side resistance in silty clay with soft and stiff consistencies, glacial clay with firm and very firm consistencies, and very firm sandy glacial clay. Table 7 presents the average SPT N and measured side resistance, q_s, for each cohesive soil type.

Table 7. Unit side resistance for cohesive soils

Type	Average SPT N	Unit Side Resistance (ksf)		
		Observed Value	Mean, μ	COV
Firm glacial clay	11–16	0.49	0.65	0.27
		0.54		
		0.69		
		0.88		
Very firm sandy glacial clay	21–34	2.88	2.73	0.59
		5.36		
		1.11		
		2.42		
		1.87		
Very firm glacial clay	28–32	1.40	1.49	-
		1.58		
Stiff silty clay	4–8	0.45	0.58	0.45
		0.85		
		0.22		
		0.58		
		0.80		
Soft silty clay	2	0.44	0.43	-
		0.42		

Mean and coefficient of variation (COV), defined as the ratio of the standard deviation for the measured resistance to the mean, are also included in the table. The sample size within this category was relatively low and ranged between two and five. The standard deviation for categories with very small sample sizes was not calculated. As observed, the largest variability in measured resistance was associated with the very firm sandy glacial clay soil. Regression analyses were conducted on the data for all cohesive soil types except for the soft silty clay and very firm glacial clay categories because these categories included only two data points. The regression analyses showed that a linear relationship exists between SPT N and unit side resistance, as shown in Figure 7 through Figure 8, although the strength of the correlation differed depending on the soil type. The goodness of the linear fit was evaluated using the coefficient of determination (R^2). For the firm glacial clay, the R^2 value was 0.6142, indicating a relatively good correlation between the two variables. For the stiff silty clay, the R^2 value when considering all five data points in the analysis was very low (i.e., 0.0197), which indicates a poor correlation between the variables. Excluding one of the data points, as shown in Figure 7b, significantly improved the R^2 to a new value of 0.8427. For the very firm glacial clay, the R^2 value was 0.1755.

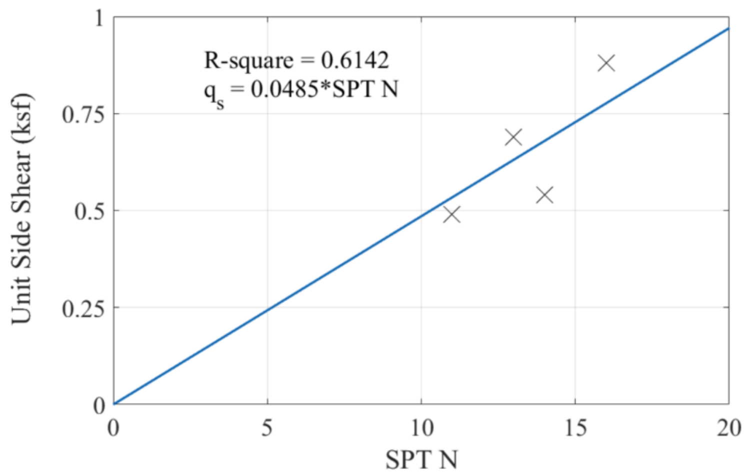

Figure 6. Unit side shear versus SPT N for firm glacial clay

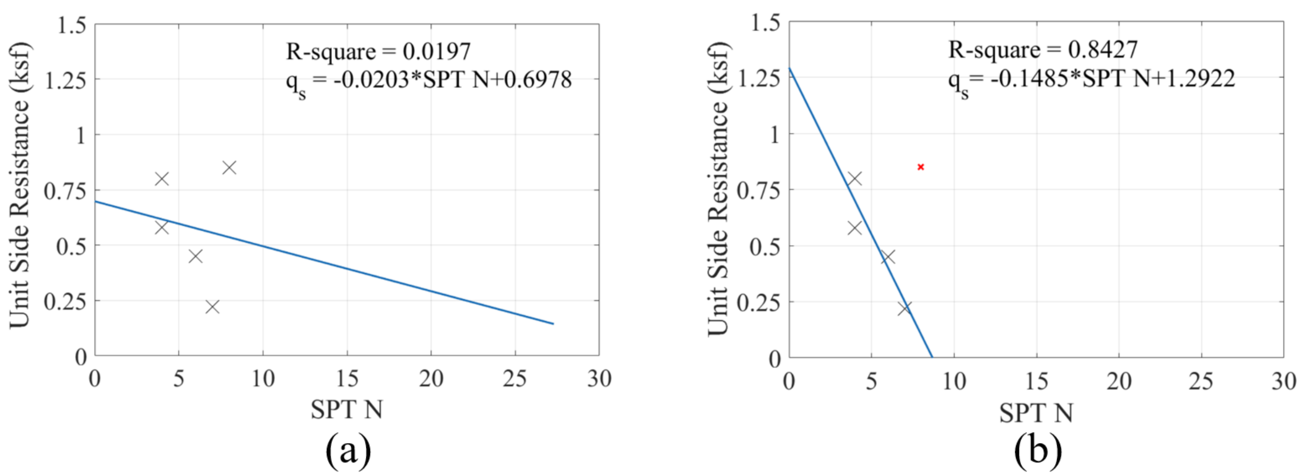

Figure 7. Unit side shear versus SPT N for stiff silty clay

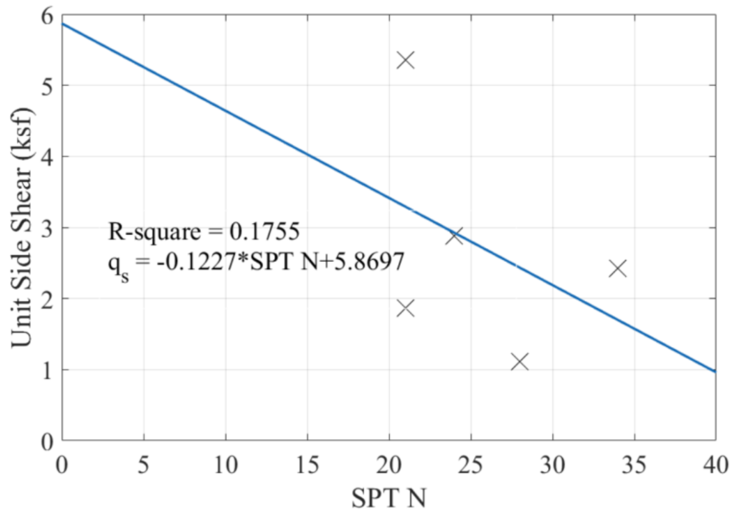

Figure 8. Unit side shear versus SPT N for very firm sandy glacial clay

3.2. Cohesionless Soils

The cohesionless soil category included 45 data points divided between fine sand, gravelly sand, coarse sand, silty sand, and granular material. Table 8 presents the SPT N, SPT N corrected for overburden and rod length (SPT N160), effective stress, and measured unit side resistance for all cohesionless soil types. Sample sizes ranged between 2 and 21, with the largest data set corresponding to the fine sand category. Regression analyses investigated the correlation between SPT N, SPT N160, σ_v, and q_s, and the results are presented in Figure 9 through Figure 20.

Table 8. Unit side resistance for cohesionless soil

Type	Average SPT N	Average SPT N160	Effective Stress at Mid-layer, σ_v (ksf)	Unit Side Resistance, q_s (ksf)		
				Observed Value	Mean, μ	COV
Fine Sand	6–27	5–23	2.41	1.42	1.83	0.64
			2.81	1.46		
			3.27	1.31		
			3.63	4.48		
			2.68	1.04		
			3.16	1.46		
			3.61	0.94		
			4.04	5.51		
			3.29	1.57		
			3.88	2.66		
			2.48	0.80		
			3.13	0.94		
			3.83	1.07		
			4.61	1.28		
			3.40	1.45		
			4.94	1.71		
			1.44	1.54		

Type	Average SPT N	Average SPT N160	Effective Stress at Mid-layer, σ_v (ksf)	Unit Side Resistance, q_s (ksf)		
				Observed Value	Mean, μ	COV
			2.02	1.56		
			2.60	2.36		
			3.13	1.55		
			4.19	2.24		
Gravelly Sand	18–30	14–24	1.62	0.81	1.05	0.43
			1.93	1.11		
			1.97	0.32		
			2.63	0.68		
			3.30	1.17		
			3.98	1.06		
			4.71	1.17		
			5.43	1.98		
			7.03	1.20		
Coarse Sand	9–27	7–22	3.87	3.94	2.09	0.41
			4.12	1.99		
			2.36	1.48		
			3.02	2.13		
			1.16	1.27		
			1.62	1.39		
			3.94	2.05		
			4.49	2.42		
Granular Material	41–63	24–43	5.32	1.73	2.35	0.26
			3.56	2.03		
			6.05	2.25		
			9.83	3.34		
			6.53	2.38		
Silty Sand	2–12	3–10	1.38	0.30	0.45	-
			1.09	0.61		

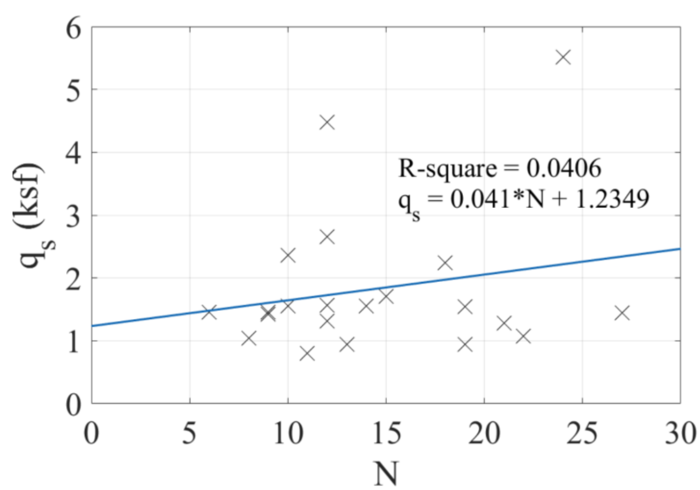

Figure 9. Unit side resistance versus N for fine sand

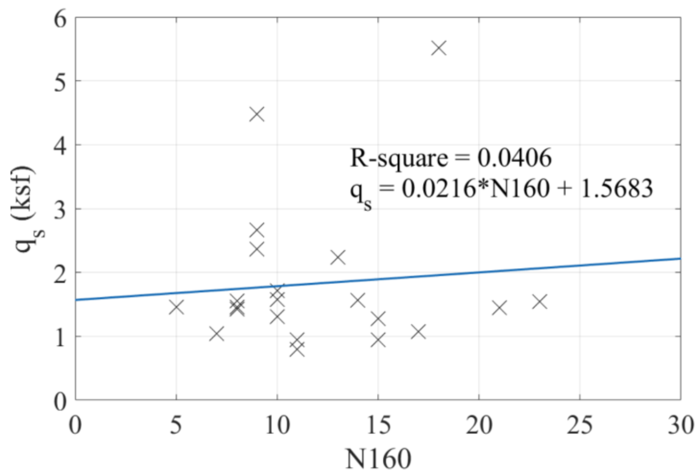

Figure 10. Unit side resistance versus N160 for fine sand

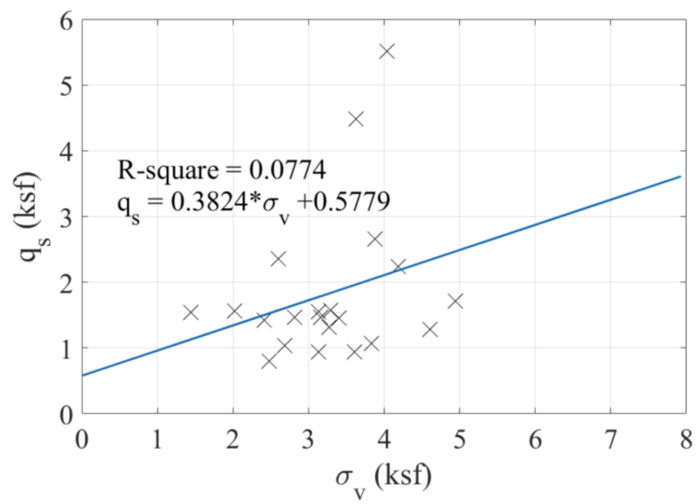

Figure 11. Unit side resistance versus effective stress for fine sand

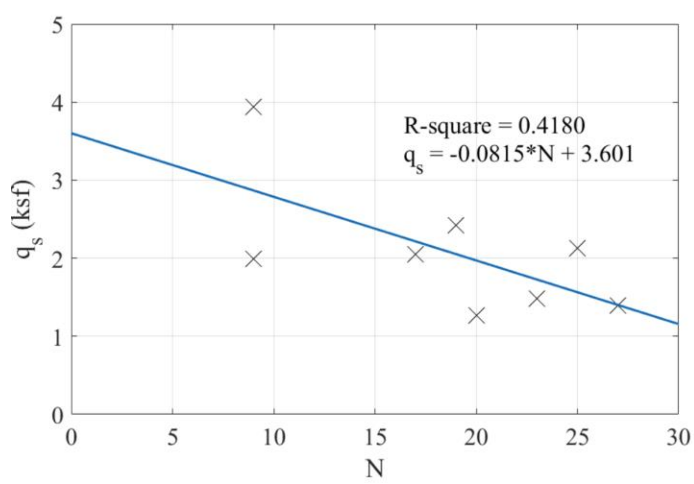

Figure 12. Unit side resistance versus N for coarse sand

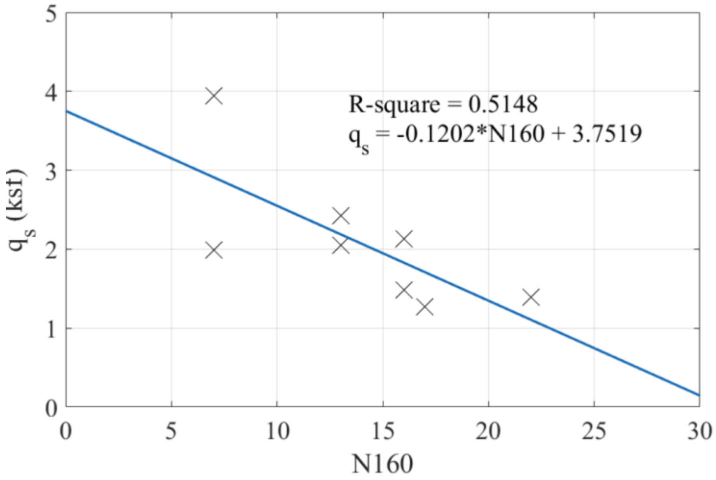

Figure 13. Unit side resistance versus N160 for coarse sand

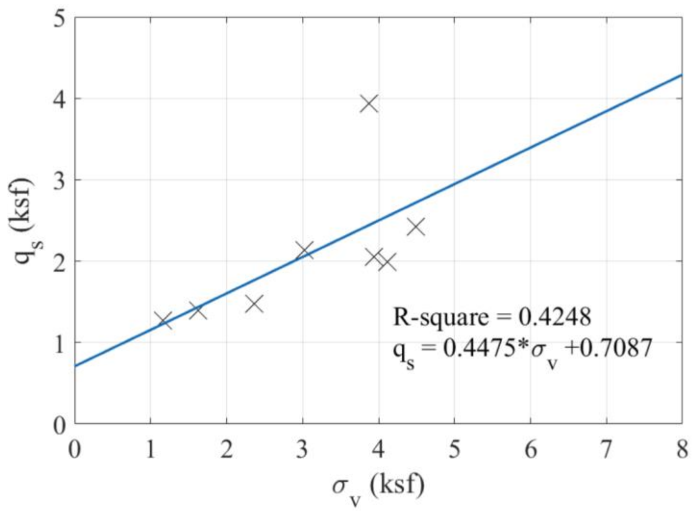

Figure 14. Unit side resistance versus effective stress for coarse sand

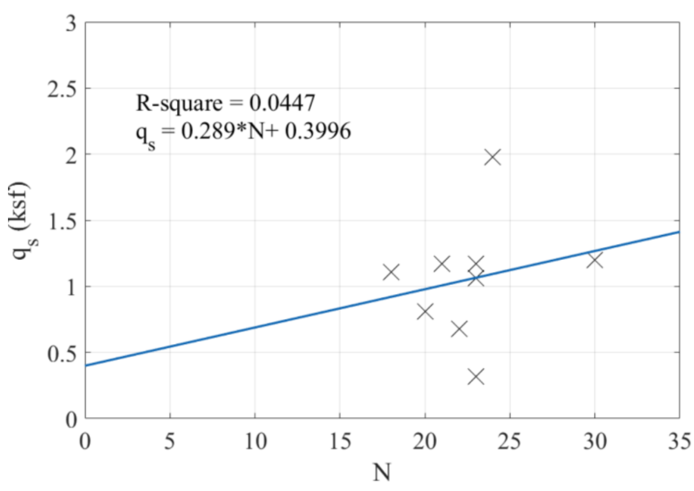

Figure 15. Unit side resistance versus N for gravelly sand

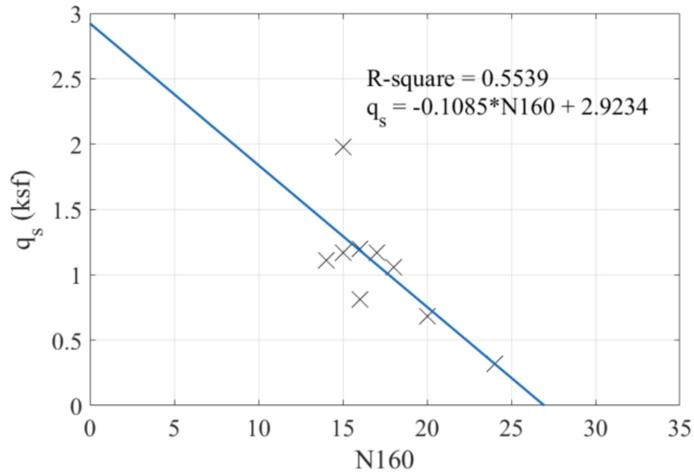

Figure 16. Unit side resistance versus N160 for gravelly sand

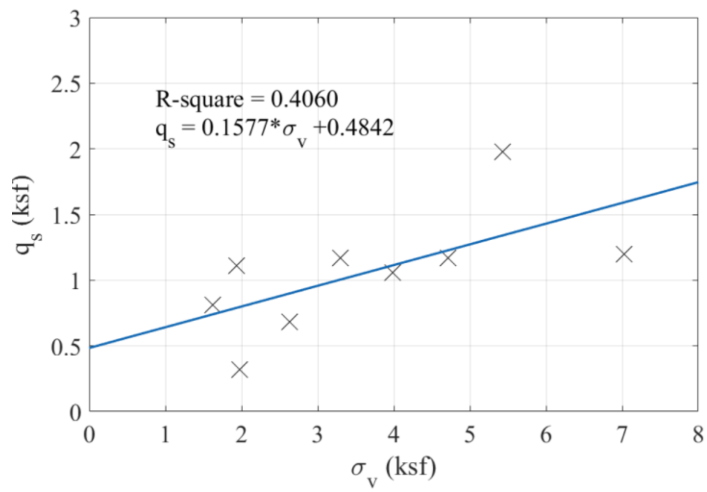

Figure 17. Unit side resistance versus effective stress for gravelly sand

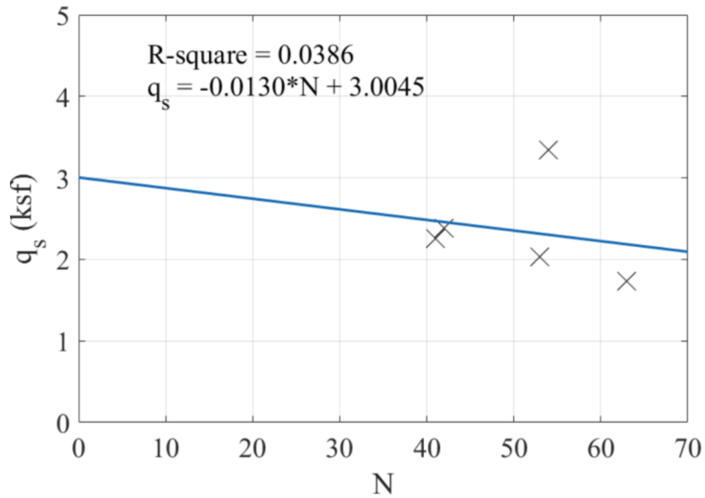

Figure 18. Unit side resistance versus N for granular material

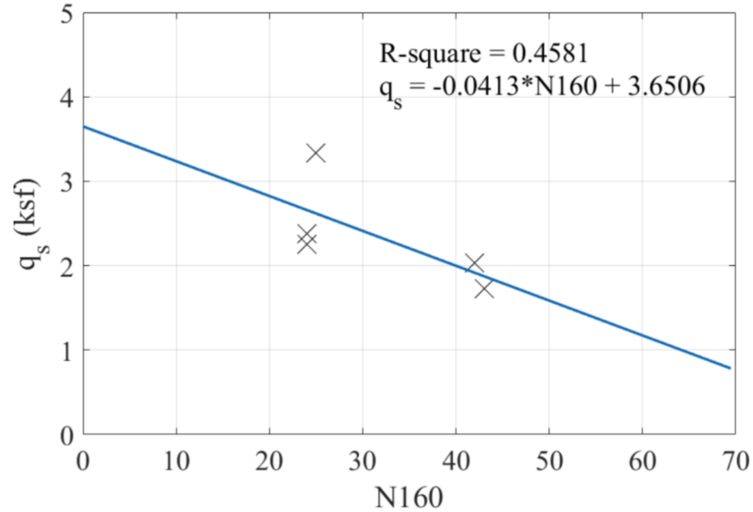

Figure 19. Unit side resistance versus N160 for granular material

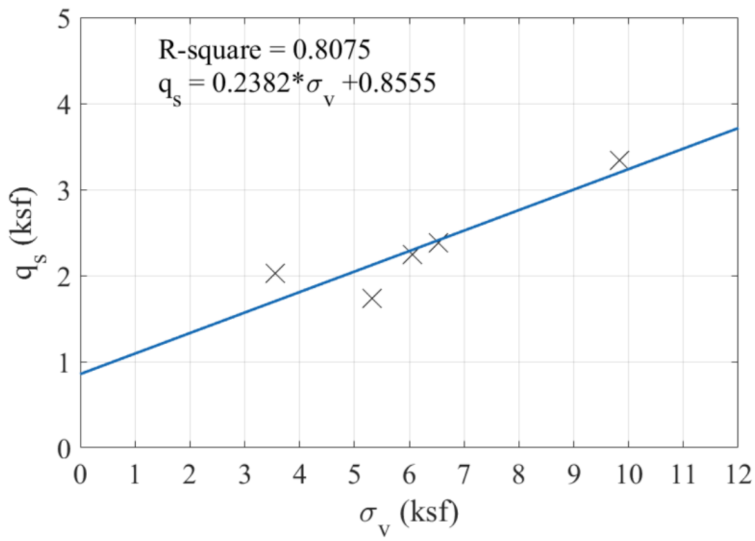

Figure 20. Unit side resistance versus effective stress for granular material

For the fine sand category, no strong correlation could be observed between soil parameters and measured resistance. The coefficient of determination for a linear fit was less than 0.1 for all investigated parameters. Relatively good linear correlations were observed for the coarse sand, gravelly sand, and granular material categories. Except for those presented in Figure 15 and Figure 18, the coefficients of determination were greater than 0.40. The strongest correlation (R^2 = 0.8075) was observed between unit side resistance and effective stress for the granular material category.

3.3. Cohesive IGM

The cohesive IGM category (i.e., 10 ksf < UCS < 100 ksf) included 10 data points of unit side resistance measured in clay shale, sandstone, and limestone. As shown in Table 9, the UCS varied between 15.89 and 93.67 ksf, and the RQD ranged between 21% and 99%.

Table 9. Unit side resistance for cohesive IGM

Type	UCS (ksf)	RQD (%)	Unit Side Resistance, q_s (ksf) Observed Value	Mean, μ	COV	Adhesion Factor, α
Clay shale	28.78	70	7.15	17.55	1.36	0.25
Clay shale	24.37	70	5.25			0.22
Clay shale	69.06	86	5.56			0.08
Clay shale	70.22	92	28.02			0.40
Clay shale	93.67	88	82.31			0.88
Clay shale	23.04	53	2.97			0.13
Clay shale/black coal	32.34	23	6.73			0.21
Fresh sandstone with thin shale seams	48.67	21	14.30			0.29
Weathered limestone with shale seams	15.89	98	9.45			0.59
Fresh sandy limestone with calcareous shale seams	41.33	99	13.80			0.33

The mean and COV of the unit side resistance were 17.55 ksf and 1.36, respectively. The adhesion factor, α, was calculated as the ratio of the measured unit side resistance to the UCS, and these values were found to vary between 0.08 and 0.88. Nonlinear regression analyses were conducted to investigate the relationship between UCS, α, and q_s. The analyses indicated a strong linear relationship between the IGM strength parameter and the measured unit side resistance, as shown in Figure 21 and Figure 22. The coefficients of determination were higher than 0.80.

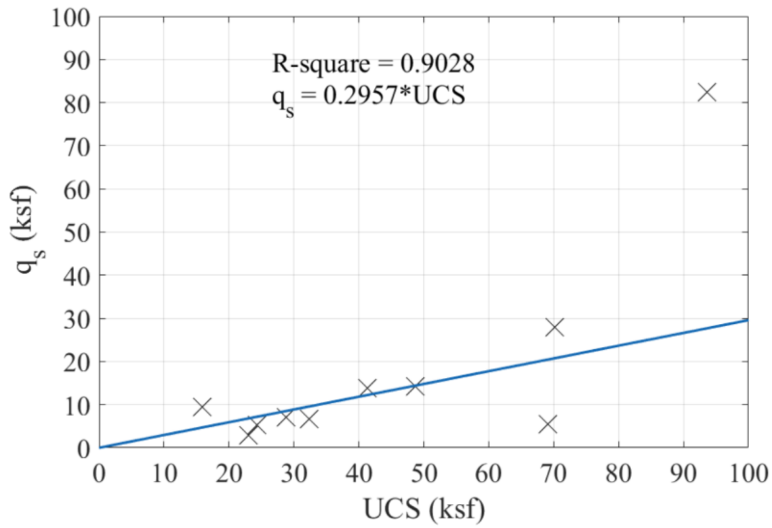

Figure 21. Unit side resistance versus UCS for cohesive IGM

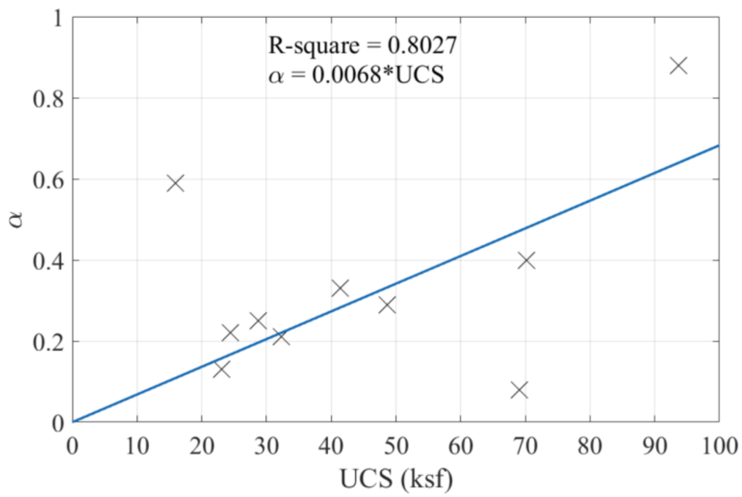

Figure 22. Adhesion factor versus UCS for cohesive IGM

3.4. Rock

The rock category (UCS > 100 ksf) included measured resistance in weathered shale, limestone, sandstone, and dolomite for a total of 18 data points. The majority of the resistance data were obtained from shaft segments in limestone and sandstone. The mean and COV were calculated for each rock type and are shown in Table 10. The COV illustrates a large variability of unit side resistance for all rock types except for weathered shale.

Table 10. Unit side resistance for rock

Type	UCS (ksf)	RQD (%)	Unit Side Resistance, q_s (ksf)			Adhesion Factor, α
			Observed Value	Mean, μ	COV	
Weathered Shale	126.41	91	19.10	18.93	0.04	0.151
	101.45	91	18.09			0.178
	129.6	66	19.61			0.153
Limestone	555.84	79	5.37	29.05	1.14	0.010
	1,388.16	79	9.26			0.007
	1,147.68	93	55.05			0.048
	938.88	100	95.19			0.101
	484.416	73	39.70			0.082
	865.08	87	35.85			0.041
Sandstone	862.56	Not given	44.42	23.95	0.55	0.051
	562.75	Not given	13.66			0.024
	259.34	64	16.37			0.063
	109.37	63	30.07			0.275
	354.74	58	15.21			0.043
Dolomite	637.2	90	41.35	56.72	0.60	0.065
	637.2	90	99.94			0.157
	637.2	90	65.14			0.102
	637.2	90	20.44			0.032

The UCS ranged between 101.45 ksf and 1,147.68 ksf. The mean and COV of the unit side resistance for all rock types were 34.12 and 0.77, respectively. Similar to the cohesive IGM category, adhesion factors were calculated, and these were found to vary between 0.007 and 0.275. Regression analyses conducted on the data set indicated that the best fit between the UCS and the measured resistance was linear, as shown in Figure 23. The estimated coefficient of determination was 0.3685. A stronger correlation was found between the adhesion factor and the UCS. As shown in Figure 24, the best correlation in this case was a power fit with a corresponding coefficient of determination of 0.608. Equations to predict the unit side resistance in rock are also shown in the aforementioned figures. Evidently, predicting the resistance in rock using the adhesion factor would produce more accurate results.

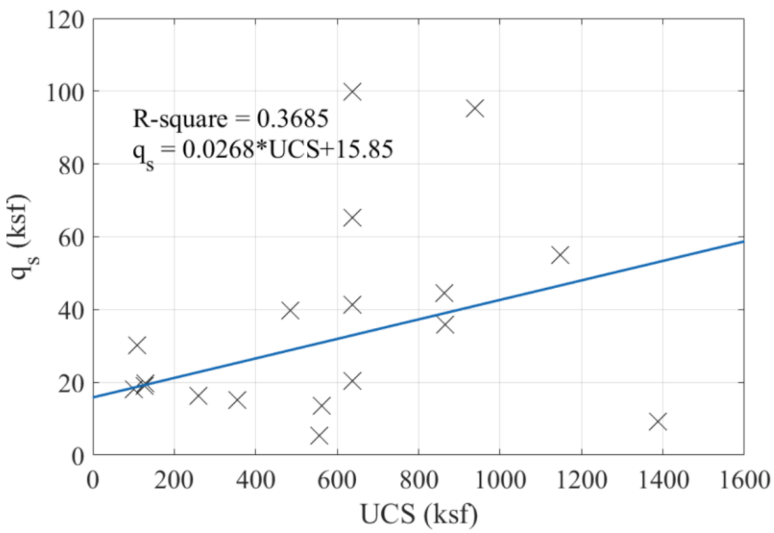

Figure 23. Unit side resistance versus UCS for rock

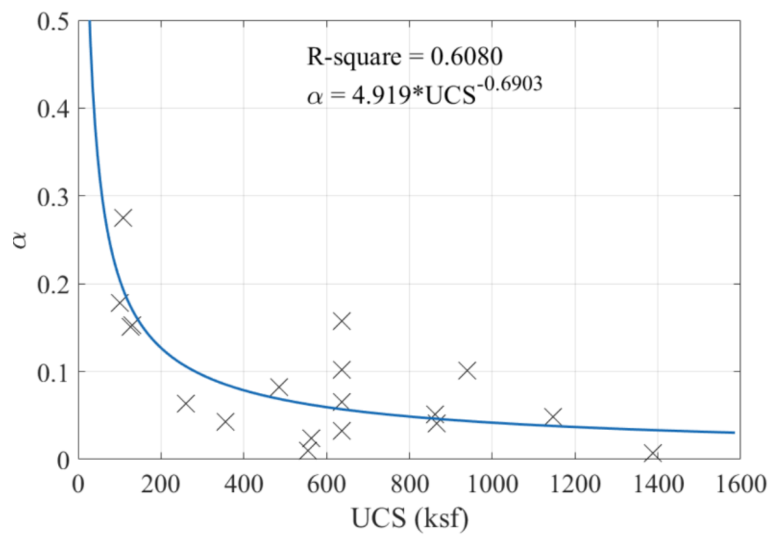

Figure 24. Adhesion factor versus UCS for rock

3.5. Load Data Analysis Conclusions

The data available in the DSHAFT database from load tests conducted in Iowa were categorized with respect to geomaterial type and analyzed to investigate existing correlations between measured geomaterial properties and unit side resistance and to develop alternative local resistance prediction methods that are more efficient than those recommended by national codes. Tables similar to those used in the Iowa DOT methodology for driven pile capacity calculation were developed based on the available data. Additionally, nonlinear regression analyses indicated that linear relationships may be appropriate to predict the unit side resistance of several of the geomaterial types investigated. The resulting equations are included in the previous sections. In some cases, the strength of the correlation was relatively poor, as indicated by low coefficients of determination. The lack of or poor correlation between the investigated parameters in some cases may be due to the fact that the unit resistance used in the analyses occurred at different shaft displacements. As mentioned above, a common criterion to define capacity could not be used in the analyses due to the limited data set. It is recommended that the database be expanded as additional load test data become available in order to evaluate the reliability of and refine the proposed methods.

CHAPTER 4. MONITORING AND ANALYSIS OF THE SETTLEMENT OF PRODUCTION SHAFTS

The intent of the analysis presented in this chapter was to evaluate the level of safety margin inherent in the current LRFD procedure used for drilled shafts, particularly in Iowa, by collecting settlement data on production shafts and performing finite element analyses to compare predicted settlements with measured settlements. To accomplish this, in collaboration with the Iowa DOT, neighboring states were contacted to secure possible construction sites for data collection. Initially, the plan was to collect settlement data from bridges constructed in Iowa and a few neighboring states, including Illinois, Minnesota, and Nebraska. However, collection of settlement data was only achieved at two bridges in Iowa due to various practical challenges. For Nebraska, reports for only two load tests at one bridge, as described in Chapter 2, were obtained.

4.1. Data Collection Sites

A brief summary of the three data collection sites, two in Iowa and one in Nebraska, is provided below.

4.1.1. Iowa

Two bridge replacement projects in Iowa were selected for the study, with drilled shafts as the proposed type of foundation for each of the project sites. The bridges were constructed across rivers with shaft foundations constructed under the bridge piers. The drilled shafts at both of the project sites in Iowa were rock socketed because the foundations hit the bedrock early.

The first project was a bridge replacement project located in Polk County, constructed along southbound IA 28 over the Racoon River. The project site had nine drilled shafts, three shafts under each pier location. The shafts had a nominal diameter of 72 in. All shafts were rock socketed and grooved.

The second project was a bridge replacement project in Franklin County, constructed along US 65 across Bailey Creek. The project site had twelve drilled shafts, including six shafts under each pier location and six shafts as a foundation for the abutment. The shafts constructed under the piers had a nominal diameter of 54 in. All shafts were rock socketed and grooved. Due to accessibility issues, the settlement in the shafts constructed under the abutment were not recorded.

The settlement in each of the drilled shafts during the various stages of construction for both projects was recorded by the Iowa DOT field surveyor.

4.1.2. Nebraska

Two Osterberg cell (O-cell) load tests were conducted as part of a major lane expansion project led by the Nebraska DOT on an 18.5-mile segment of the US 275 expressway located between Scribner and West Point. The site of this project is referred to as the Scribner North site.

Unlike the Iowa DOT, the Nebraska DOT was only able to provide load test data for test shafts drilled as part of the bridge project. Settlement data were not collected during the various phases of bridge construction, as had been performed for the projects in Iowa. Instead, a numerical analysis using PLAXIS was conducted to predict settlement.

4.2. Methodology

The objective of this task was to observe and record the axial displacements at the tops of the shafts as the shaft axial loads were increased during the various stages of construction of the bridge components. The displacements were recorded at the shaft tops using surveying instruments. Table 1 presents the plan for recording the displacements occurring at the shaft tops during each stage of construction of the bridge components.

Table 11. Stages for recording shaft head elevation via surveying

Stage	Structure	Measurements Recorded
1	Drilled Shaft Construction	• The elevation of the top of the shaft was measured and recorded after the concrete was poured at the location. • Measurements from two diametrically located points on the shaft top were preferred.
2	Pier/Column Construction with Pier Cap	• The elevation of the shaft top was measured after construction of the pier and the pier cap. • If the shaft top was not visible, then the elevation was measured based on a target point on the substructure above the shaft (e.g., column).
3	Bridge Superstructure Construction	• The elevation of the shaft top (if visible) or of a target point on substructure was measured and recorded after placement of major bridge components (e.g., beams, girders, deck)
4	Open to Traffic	• Data were collected after the bridge was opened to traffic, preferably at 6 months, 1 year, and beyond.

Figure 25 and Figure 26 show a schematic representation of the target points at which the elevation measurements were recorded during the various stages of construction at each of the project sites.

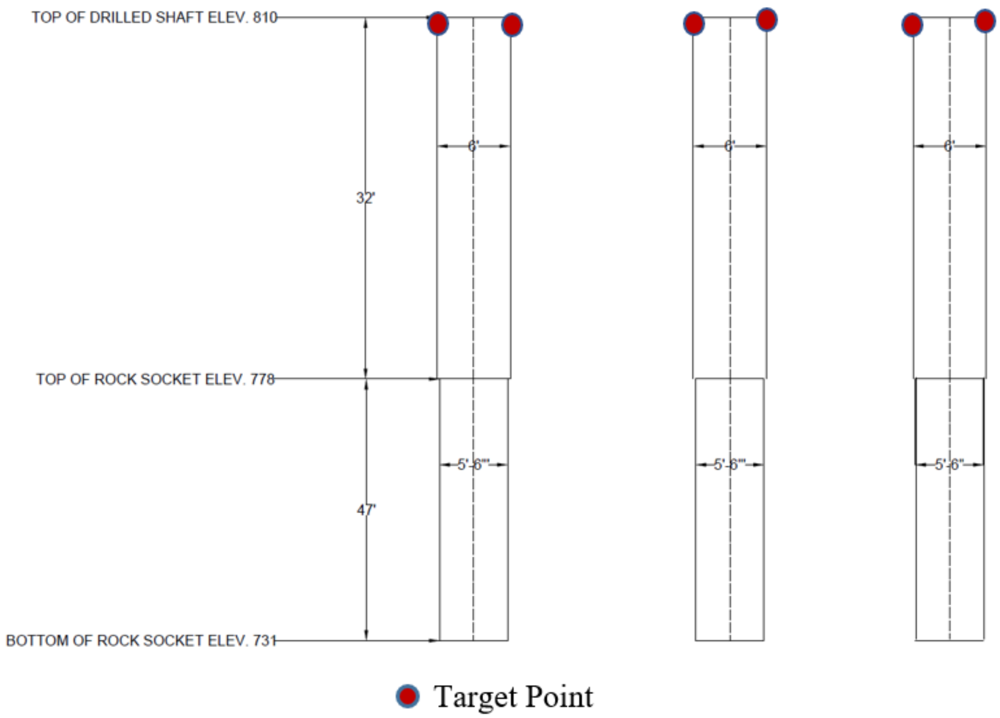

Figure 25. Elevation measurements after construction of drilled shafts (Stage 1)

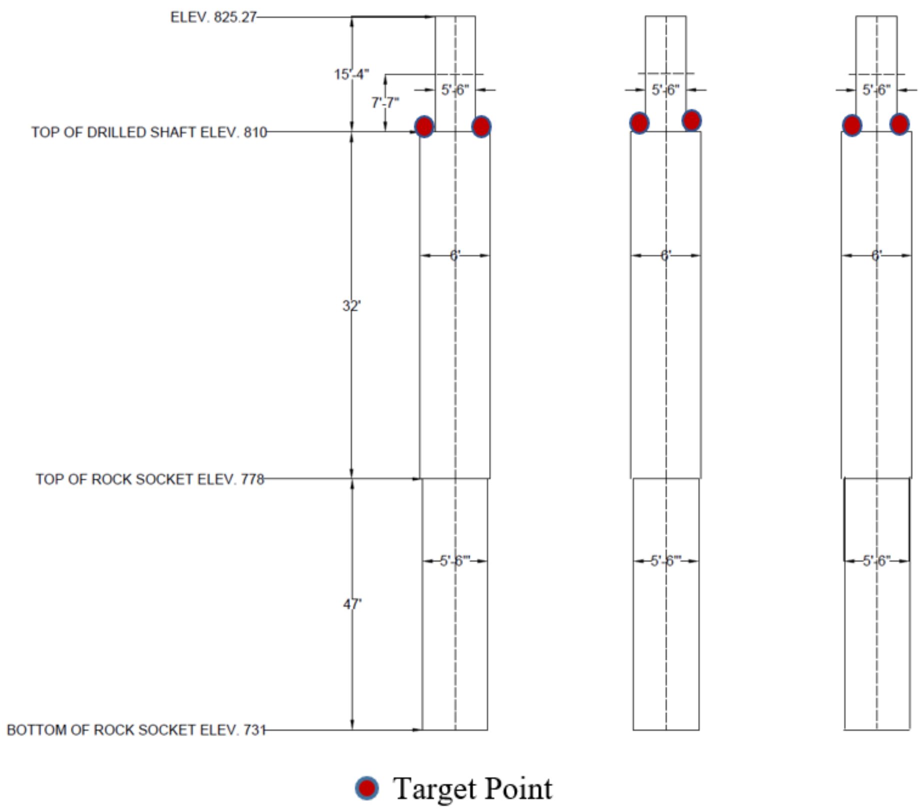

Figure 26. Elevation measurements after construction of pier with pier cap (Stage 2)

4.3. Data Collection

At each project site, displacements at the shaft tops were recorded by an Iowa DOT field surveyor using a surveying instrument. Specifically, two types of surveying instruments were utilized to record the displacements at the shaft heads. A robotic total station with a glass prism was used to record the displacements at the Polk County bridge replacement project, whereas a rod and pole surveying technique was used at the Franklin County bridge replacement project. Specific areas at the tops of the shafts were scraped and polished to obtain a smooth surface on which to record the elevation measurements.

The nomenclature adopted for the shafts at each of the project sites was different. The shafts at the Polk County project site were named based on the pier number and the direction relative to north followed by the diametric position. For example, P1 W1 means that the elevation was recorded at the top of the drilled shaft at Point 1 (diametrically opposite to Point 2) constructed in the west direction under the Pier 1 location. The shafts at the Franklin County project site were named based on the pier number and the direction relative to north. For example, P1 W means that the elevation was recorded at the top of the shaft placed under Pier 1 in the west direction, and P1M stands for the elevation recorded at the top of the middle shaft placed under Pier 1.

Figure 27 shows the completed drilled shafts after curing of the concrete at the Polk County project site. Figure 28 and Figure 29 show the locations of the shafts in the west and east directions under each pier at the project site located in Franklin County.

Figure 27. Completed drilled shaft construction, Polk County

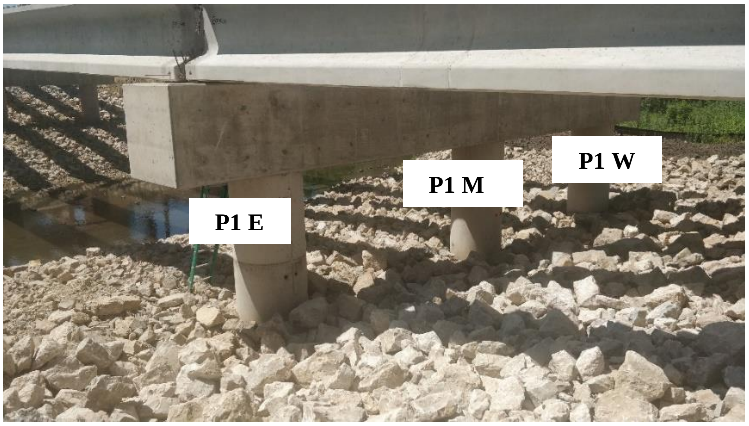

Figure 28. Drilled shafts after placement of pier cap and girders, Franklin County

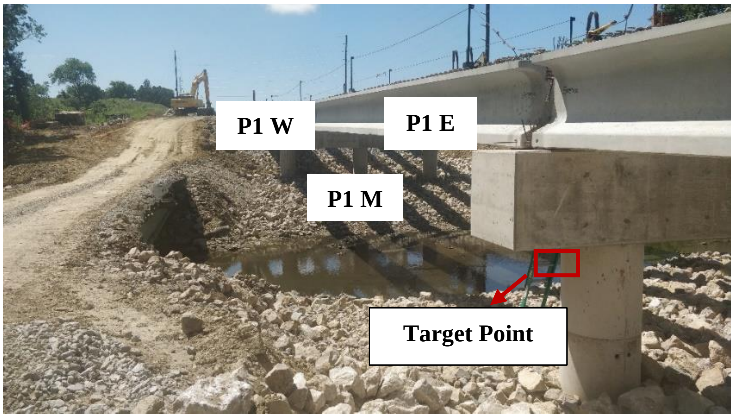

Figure 29. Location of shaft head elevation measurement, Franklin County

Figure 30 and Figure 31 show the location of Piers 1 and 2 at the Polk County bridge project site and the location of the point at which elevation was measured at the drilled shaft tops. Figure 32 shows a robotic total station being used to record the elevation of a shaft head at the Polk County project site.

Figure 30. Girders and piers constructed over the shafts, Polk County

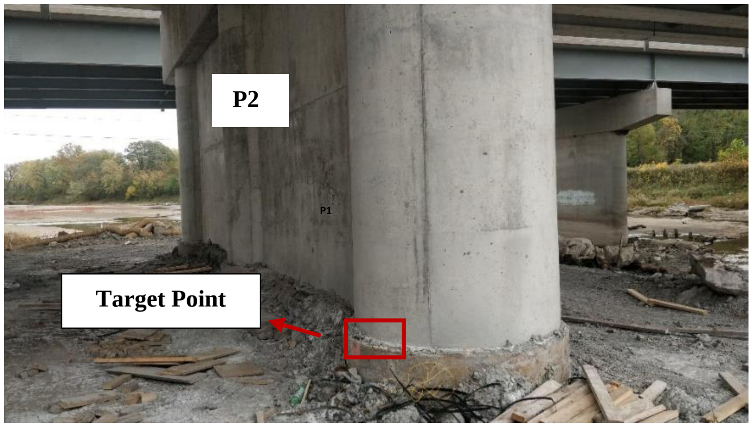

Figure 31. Location of shaft head elevation measurement, Polk County

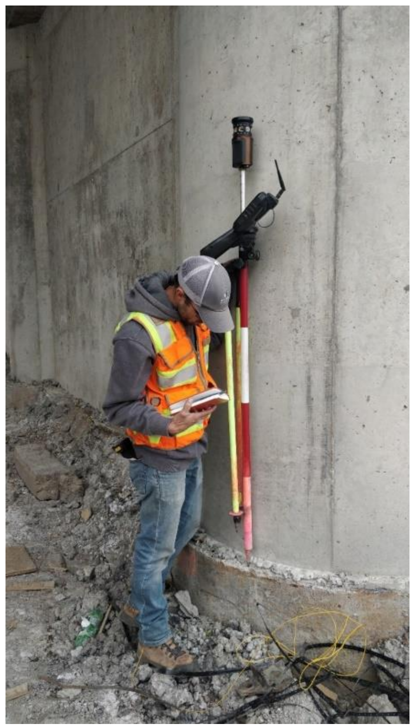

Figure 32. Robotic total station used to record elevation, Polk County

Table 12 and Table 13 indicate the elevation measurements recorded via surveying during the various stages of bridge construction at each of the bridge replacement project sites.

Table 12. Elevations recorded at Polk County project site

Pier Number	Initial Elevation (ft)	Elevation with Pier Cap (ft)	Elevation with Girders (ft)	Elevation after Deck Pour (ft)	Settlement after Pier Cap (in.)	Settlement after Girder Placement (in.)	Settlement after Deck Pour (in.)	Total Settlement (in.)	Average Settlement in Each Pier (in.)
P1 E1	810	809.989	809.951	809.915	0.132	0.456	0.432	1.020	0.930
P1 E2	810	810.023	**	809.930	-0.276	-	-	0.840	
P1 M1	810	810.027	809.991	809.950	-0.324	0.432	0.492	0.600	0.444
P1 M2	810	810.046	810.064	809.976	-0.552	-0.216	1.056	0.288	
P1 W1	810	809.989	809.940	809.908	0.132	0.588	0.384	1.104	1.086
P1 W2	810	810.001	810.000	809.911	-0.012	0.012	1.068	1.068	
P2 E1	803	803.018	**	802.934	-0.216	-	-	0.792	0.858
P2 E2	803	803.039	803.022	802.923	-0.468	0.204	1.188	0.924	
P2 M1	803	803.023	802.969	802.930	-0.276	0.648	0.468	0.840	1.086
P2 M2	803	802.992	**	802.889	0.096	-	-	1.332	
P2 W1	803	803.025	802.947	802.910	-0.300	0.936	0.444	1.080	1.056
P2 W2	803	803.014	803.013	802.914	-0.168	0.012	1.188	1.032	
P3 E1	803	802.999	803.011	802.936	0.012	-0.144	0.900	0.768	0.444
P3 E2	803	803.033	**	802.990	-0.396	-	-	0.120	
P3 M1	803	802.941	802.891	802.909	0.708	0.600	-0.216	1.092	1.158
P3 M2	803	802.925	**	802.898	0.900	-	-	1.224	
P3 W1	803	802.939	802.974	802.928	0.732	-0.42	0.552	0.864	0.594
P3 W2	803	802.976	803.070	802.973	0.288	-1.128	1.164	0.324	

** No data collected

Table 13. Elevations recorded at Franklin County project site

Pier Number	Initial Elevation (ft)	Elevation With Pier Cap (ft)	Elevation with Beams (ft)	Elevation with Deck Pour (ft)	Settlement after Pier Cap Construction (in.)	Settlement after Beam Placement (in.)	Settlement after Deck Pour (in.)	Total Settlement (in.)	Average Settlement in Each Pier (in.)
P1 E	1,067.22	1,067.23	1,067.22	1,067.24	-0.12	0.12	-0.24	-0.24	
P1 M	1,067.22	1,067.23	1,067.22	1,067.23	-0.12	0.12	-0.12	-0.12	-0.20
P1 W	1,067.22	1,067.25	1,067.24	1,067.24	-0.36	0.12	-	-0.24	
P2 E	1,064.19	1,064.15	1,064.14	1,064.14	0.48	0.12	-	0.60	
P2 M	1,064.19	1,064.16	1,064.15	1,064.14	0.36	0.12	0.12	0.60	0.48
P2 W	1,064.19	1,064.17	1,064.16	1,064.17	0.24	0.12	-0.12	0.24	

From the shaft top elevation data, it was observed that settlement was recorded as a negative value at certain shaft locations, indicating that the shaft experienced an uplift instead of settlement after the construction of different components of the bridges. More data are advised to be collected to understand this phenomenon. At certain locations at the Polk County project site, the shaft top elevations could not be recorded due to poor visibility and the limitations of the surveying instruments.

4.4. Numerical Modeling of a Drilled Shaft at the Scribner North Site

A two-dimensional numerical model was developed in PLAXIS to predict the settlement at the top of a drilled shaft under axial loading. The results obtained from the numerical model were then compared with the equivalent top load-displacement curve generated from the O-cell report for the test shaft at the Scribner North site. The purpose of this study was to understand whether the numerical model is able to accurately predict the load-displacement behavior of the test shaft under working loads and to use the model to evaluate the level of conservativeness of the methods used to design the shaft.

4.4.1. Numerical Modeling

The test shaft was located at the Scribner North site in Nebraska. The soil at the site consisted of fat and lean clay with a consistency ranging from hard to firm within the first 20 ft below the ground surface. From a depth of 20 to 46 ft, the soil was characterized by silty sand deposits with a density ranging from loose to medium. Below a depth of 46 ft, the soil was classified as a fat clay deposit with a consistency ranging from hard to very hard. The water table at the site was at a depth of 12 ft below the ground surface.

The test shaft had a nominal diameter of 67 in. with a permanent casing along the top 8 ft of the shaft. The remainder of the shaft had a reduced nominal diameter of 60 in. The length of the shaft was approximately 90 ft. The test shaft was a floating shaft with the base located in fat clay from the Nebraskan glacial till. Figure 33 shows a schematic diagram of the test shaft and the surrounding soil layers that was adopted in the PLAXIS model.

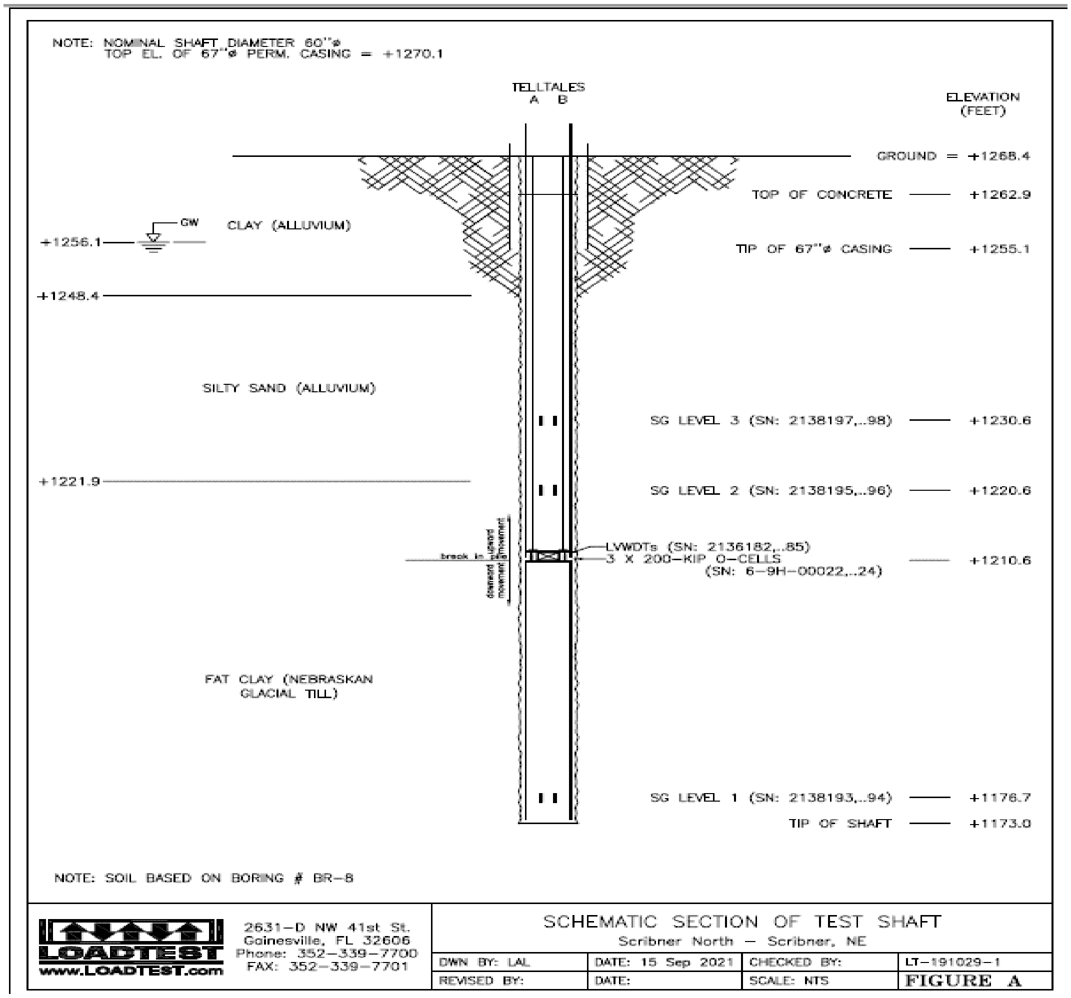

Figure 33. Test shaft constructed at the Scribner North site

4.4.2. Numerical Model Results and Comparison with Equivalent Top Load-Displacement Data

A bi-directional O-cell test was conducted on the test shaft. An equivalent top load curve was calculated and reported in the load test report. From the equivalent top load-displacement data based on the O-cell test, it was observed from the extrapolated data that at a working load of 1,100 kips, the shaft would have a top displacement of 0.22 in., which is close to the service limit state criterion of 0.25 in. (Iowa DOT 2024). The settlement of the shaft was then empirically calculated based on the shaft and end bearing resistance guidelines stated in the *AASHTO LRFD Bridge Design Specifications* (AASHTO 2017). The unit shaft resistance in cohesive soil was calculated based on the alpha method by Tomlinson (1971), and in cohesionless soil the shaft resistance was calculated based on a method by Chen and Kulhawy (2002). The unit base resistance was calculated based on the bearing capacity factor and the undrained shear strength of cohesive soil. The factored shaft and base resistances were then calculated based on the resistance factor adopted for each layer. The settlement occurring in the shaft due to the application of axial loads was calculated based on a normalized load-displacement curve adapted from Chen and Kulhawy (2002) for the nominal shaft resistance values. The settlement calculated in the shaft due to the application of axial loads based on an empirical chart adapted from Chen and Kulhawy (2002) is plotted in Figure 35. The shaft was predicted to reach its serviceability state under an axial load of 1,000 kips with a corresponding displacement of 0.23 in.

A numerical model of the shaft was then created in PLAXIS (Figure 34), and the capacity of the shaft under the service limit state was studied. Appropriate soil properties characterizing the real site conditions were adopted in the model. The fat clay layers were characterized by undrained shear strengths, and the silty sand layers were characterized based on the preconsolidation stress and soil friction angle values. The values of undrained shear strength, preconsolidation stress, and soil friction angle were calculated based on the standard penetration test *N* value obtained from the boring log report available for the bridge site. The test shaft was characterized by a concrete unit weight of 145 lb/ft^2, as used under actual testing conditions. The settlement at the top of the shaft was evaluated at axial loads ranging from 0 kips to 2,000 kips.

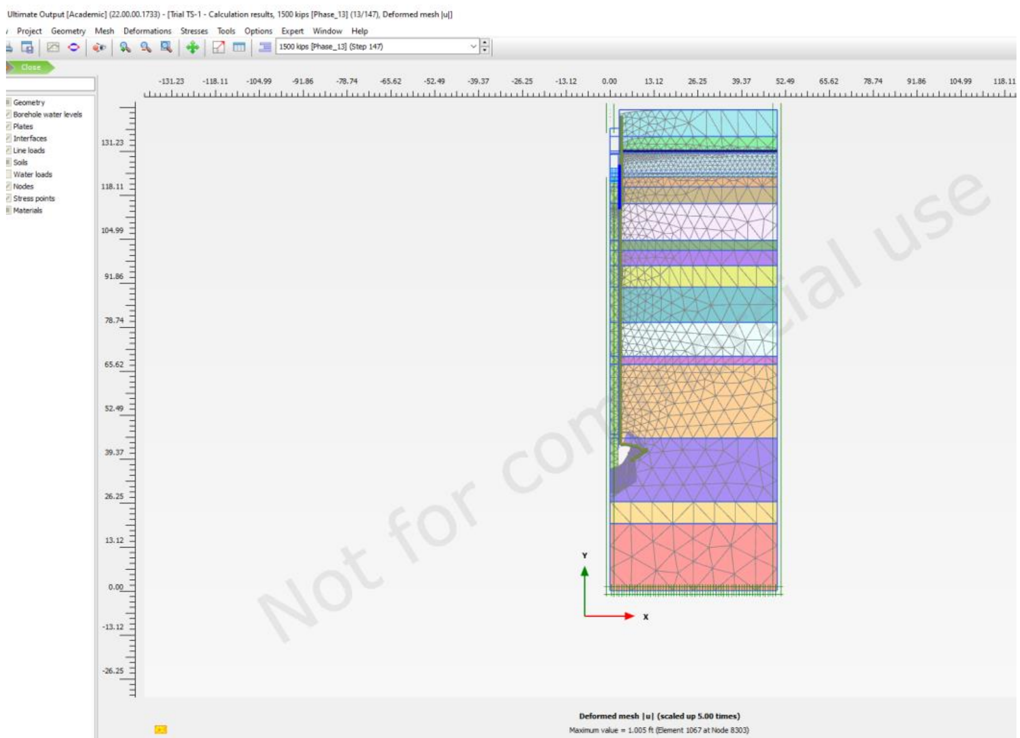

Figure 34. PLAXIS model

In the PLAXIS model, the drilled shaft was completely mobilized at an axial load of 1,200 kips. The shaft capacity was reached at 1,200 kips, with a displacement of 0.25 in. recorded under the working load for the test shaft. Figure 35 plots the settlement in the shaft under a range of axial loads. Both the empirical calculations and the numerical model predict the service limit state under a working load of 1,200 kips, with a displacement of around 0.25 in. recorded at the top of the shaft. These data are in agreement with the extrapolated top load-displacement data generated from the bi-directional test data.

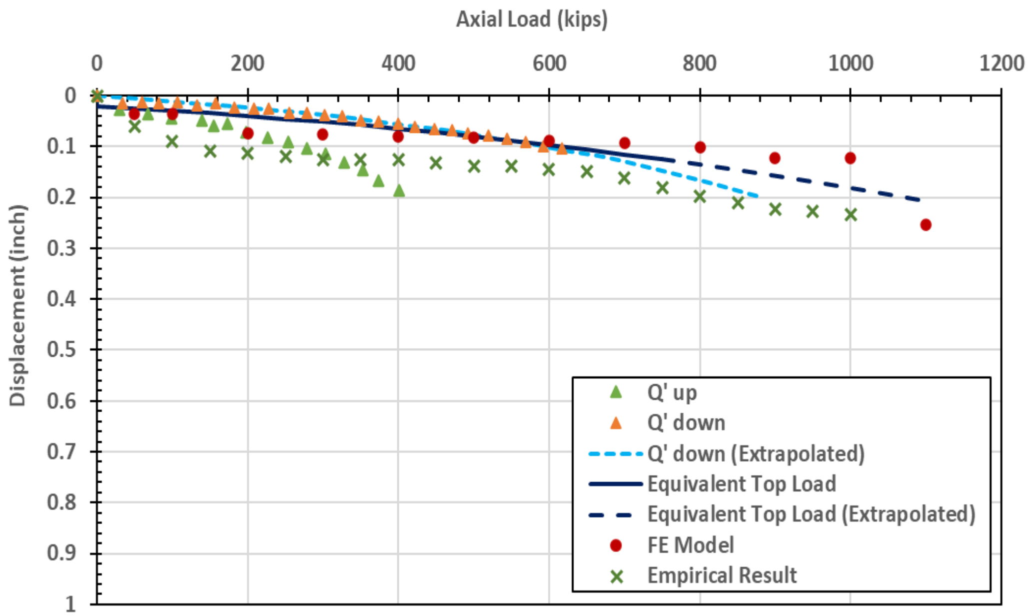

Adapted from load test report for the Scribner North site, 2021

Figure 35. Settlement of the test shaft under axial loads

4.5. Conclusions from Monitoring and Analysis of the Settlement of Production Shafts

Shaft top elevation data from two bridge replacement projects in Iowa with drilled shaft foundations were recorded using surveying instruments. The data collected were utilized to calculate settlement at the shaft tops after construction of each bridge component. Primarily, settlement at the shaft tops was calculated between construction of the shaft and construction of the piers and pier caps, after construction of the beams, and after pouring of the bridge deck. Total settlement was also calculated based on the elevation of the shaft top just after shaft construction, just after pouring of the concrete, and after pouring of the bridge deck and rails.

In the settlement values calculated, some of the shafts indicate negative settlement/uplift values. This could be due to human errors incurred during surveying or due to a phenomenon that needs to be investigated further. At some locations, it was difficult to collect shaft top elevation data because poor weather conditions reduced the visibility and accuracy of the surveying instrument.

Several challenges arose during shaft construction, and hence it is recommended to choose appropriate benchmark points at which data can be recorded accurately and to record the elevation of the shafts at multiple points on the shaft tops. Differential settlement in the shafts can be detrimental to the superstructure, and hence it is advised that future studies collect more elevation data points at the shaft tops because there is immense value in using data recorded along the lengths of the bridge and across multiple shafts to identify differential settlements along the superstructure. Several challenges were experienced due to inclement weather and a lack of accessibility to shaft tops that were built in the path of a river, and as a result the data set is very limited. For future studies predicting the capacity of drilled shafts under the service limit state, it is recommended that more elevation data points at the shafts be recorded. It is also recommended to track the elevation of the shaft tops after the bridges are opened to traffic at intervals of 6 months, 1 year, and beyond.

Data collected from the project sites in Iowa will help the engineering community understand the settlement behavior of drilled shafts during construction and after opening to traffic. Settlement data recorded with the assistance of survey tools and numerical models will improve predictions of drilled shaft capacity and the design of drilled shafts based on a service state criterion of 0.25 in. maximum displacement. Using better predictions and designs will prove to be faster and more economical than conducting a field test on a test shaft.

CHAPTER 5. DESIGN RECOMMENDATIONS

Based on the findings of Kalmogo et al. (2019) and those of this project, the following recommendations are made for the design of axially loaded drilled shafts in the state of Iowa. The recommendations presented in this chapter are illustrated through design examples in the appendix to this report.

The basic LRFD relationship used to determine the contract length for an individual drilled shaft is the following:

$R_R = R_{sR} + R_{pR} \geq \gamma Q$ (consistent units of force)

where

R_R = factored axial shaft resistance (consistent units of force),
R_{sR} = factored side resistance (consistent units of force),
R_{pR} = factored tip resistance (consistent units of force), and
γQ = factored load for the appropriate strength limit state (consistent units of force).

Tip resistance and side resistance shall be computed according to the provisions of this chapter for the material type(s) encountered.

The factored side resistance for drilled shafts shall be established from factored unit side resistance values for the relevant soil/rock conditions as provided in this chapter. For stratified ground conditions or where the shaft dimensions change (e.g., at the tip of temporary or permanent casing or at the top of a rock socket), the shaft shall be divided into segments with practically uniform shaft geometry and soil/rock properties and unit side resistance values determined for each shaft segment. The total factored side resistance shall then be computed as the sum of the factored resistance values for each shaft segment:

$$R_{sR} = \sum_{i=1}^{n}(q_{sR-i} \cdot A_{s-i}) = \sum_{i=1}^{n} \varphi_{qs-i} \cdot q_{s-i} \cdot \pi \cdot D_i \cdot L_i \qquad (1)$$

where

n = number of shaft segments,
q_{sR-i} = $\varphi_{qs-i} \cdot q_{s-i}$ = factored unit side resistance for shaft segment i (consistent units of stress),
A_{s-i} = $\pi \cdot D_i \cdot L_i$ = shear area for shaft segment i (consistent units of area),
φ_{qs-i} = resistance factor for unit side resistance along shaft segment i (dimensionless),
q_{s-i} = nominal unit side resistance along shaft segment i (consistent units of stress),
D_i = shaft diameter for shaft segment i (consistent units of length), and
L_i = length of shaft segment i (consistent units of length).

φ_{qs-i} and q_{s-i} shall be determined in accordance with the recommendations in this chapter, based on the geomaterial type present along the respective shaft segment.

Side resistance shall generally be neglected or reduced, as recommended by the Geotechnical Section, over shaft segments with permanent casing and over any length of rock socket that is deemed unusable.

The factored tip resistance for drilled shafts shall be established from factored unit tip resistance values for the relevant soil/rock conditions as provided in this chapter. The appropriate tip resistance shall be established for the soil/rock located between the tip of the shaft and two diameters below the tip of the shaft. The factored tip resistance shall be computed as follows:

$$R_{pR} = q_{pR} \cdot A_p = \varphi_{qp} \cdot q_p \cdot \pi \cdot \frac{D^2}{4} \tag{2}$$

where

q_{pR} = $\varphi_{qp} \cdot q_p$ = factored unit tip resistance (consistent units of stress),
Ap = $\pi \cdot \frac{D^2}{4}$ = cross-sectional area of the shaft at the tip (consistent units of area),
φ_{qp} = resistance factor for unit tip resistance (dimensionless),
q_p = nominal unit tip resistance (consistent units of stress), and
D = shaft diameter at the tip of the shaft (consistent units of length).

φ_{qp} and q_p shall be determined in accordance with the recommendations in this chapter, based on the material type present within a depth of $2D$ below the tip of the shaft.

The specific design methods and resistance factors for determining nominal and factored side and tip resistance shall be selected based on the material type(s) present along the sides and below the tip of the shaft as specified in the following sections:

- Section 5.1 shall generally be followed for determining nominal and factored side and tip resistance in cohesive soils with an undrained shear strength (s_u) of less than 5 ksf.
- Section 5.2 shall generally be followed to estimate resistance for shafts in cohesionless soils and IGM.
- Section 5.3 shall generally be followed to estimate shaft resistance in cohesive IGMs with a rock strength ranging between 10 ksf and 100 ksf measured from uniaxial compression tests on intact rock core samples.
- Section 5.4 shall generally be followed to determine shaft resistance in rock with a strength greater than 100 ksf as measured from uniaxial compression tests on intact rock core samples.

5.1. Axial Resistance for Individual Drilled Shafts in Cohesive Soils (su ≤ 5 ksf)

The nominal unit side resistance for shaft segments located in cohesive soils shall be computed from undrained shear strength correlated to SPT blow count number using the O'Neill and Reese (1999) α-method as follows:

$$q_s = \alpha \cdot s_u \tag{3}$$

where

q_s = nominal unit side resistance for the shaft segment,
α = an empirical coefficient (dimensionless), and
s_u = mean value of the undrained shear strength for the soil along the shaft segment.

The value of α shall be taken as follows:

α = 0 between the ground surface and a depth of 5 ft or to the depth of seasonal moisture change, whichever is greater,
α = 0.55 along the shaft segment for $\frac{s_u}{p_a} \leq 1.5$,
α $= 0.55 - 0.1\left(\frac{s_u}{p_a} - 1.5\right)$ along the shaft segment for $1.5 \leq \frac{s_u}{p_a} \leq 2.5$, and
p_a = atmospheric pressure in the same unit as s_u (2.12 ksf or 14.7 psi in US customary units).

The value of s_u shall be determined from the average uncorrected blow count N along the shaft segment using Table 14.

Table 14. Undrained shear strength correlation to SPT blow count number

s_u, ksf	0	0.25	0.5	1	2	4
N, standard penetration resistance	0	2	4	8	16	32

Source: Bowles 1982

The resistance factor (φ_{qs}) to be applied to the nominal resistance value (q_s) determined according to equation (3) shall be taken as 0.50.

The nominal tip resistance for shafts tipped in cohesive soils shall be calculated using the following expression by O'Neill and Reese (1999):

$$q_p = N_c \cdot s_u \leq 80.0\ ksf \tag{4}$$

where

q_p = nominal unit tip resistance for the shaft,
s_u = mean undrained shear strength of the cohesive soil over a depth of 2B below the base, and
N_c = bearing capacity factor (dimensionless).

The value for N_c shall be taken as follows:

$$N_c = 6\left[1 + 0.2\left(\frac{Z}{D}\right)\right] \leq 9 \tag{5}$$

where

Z = depth of the tip of the shaft from the ground surface (consistent units of length), and
D = shaft diameter (consistent units of length).

The value for N_c predicted using equation (5) shall be limited to a maximum value of 9.0. For $s_u \leq 0.5\ ksf$, N_c shall be multiplied by 0.67.

Unless greater resistance can be verified by a load test, the nominal unit tip resistance predicted using equation (4) shall be limited to a maximum value of 80 ksf.

The resistance factor (φ_{qp}) to be applied to the nominal resistance value (q_p) determined according to equation (4) shall be taken as 0.40 as recommended by AASHTO (2017).

5.2. Axial Resistance for Individual Drilled Shafts in Cohesionless Soils and IGM

The nominal unit side resistance for shaft segments located in cohesionless soils and IGM shall be computed using the O'Neill and Reese (1999) β-method as follows:

$$q_s = \beta \cdot \sigma_v' \tag{6}$$

where

q_s = nominal unit side resistance for the shaft segment,
β = an empirical correlation factor (dimensionless), and
σ_v' = average vertical effective stress for the soil along the shaft segment.

The value of β shall be calculated as follows:

$$\beta = 1.5 - 0.135\sqrt{z} \qquad \text{for } N_{60} \geq 15 \qquad 0.25 \leq \beta \leq 1.20 \tag{7}$$

$$\beta = \frac{N_{60}}{15}\left(1.5 - 0.135\sqrt{z}\right) \text{for } N_{60} < 15 \qquad 0.25 \leq \beta \leq 1.20 \tag{8}$$

The resistance factor (φ_{qs}) to be applied to the nominal unit side resistance shall be taken as 0.75 for cohesionless soils and for cohesionless IGM.

The nominal unit tip resistance for shafts founded on cohesionless soils shall be determined from corrected SPT N values, N_{60} (O'Neill and Reese 1999).

$$q_p = 1.2 \cdot N_{60} \leq 60\ ksf \tag{9}$$

where

q_p = nominal unit tip resistance for the shaft (ksf), and
N_{60} = average SPT N value corrected for hammer efficiency (blows/ft).

The resistance factor (φ_{qp}) shall be taken as 0.50 as recommended by AASHTO (2017).

5.3. Axial Resistance for Individual Drilled Shafts in Cohesive IGM

The nominal unit side resistance for shaft segments located in cohesive IGM shall be computed from measurements of uniaxial compressive strength on rock cores as follows:

$$q_s = \alpha \cdot \phi \cdot q_u \tag{10}$$

where

α = empirical factor determined from Figure 36,
ϕ = a correction factor to account for the degree of jointing, and
q_u = uniaxial compressive strength of intact rock (ksf).

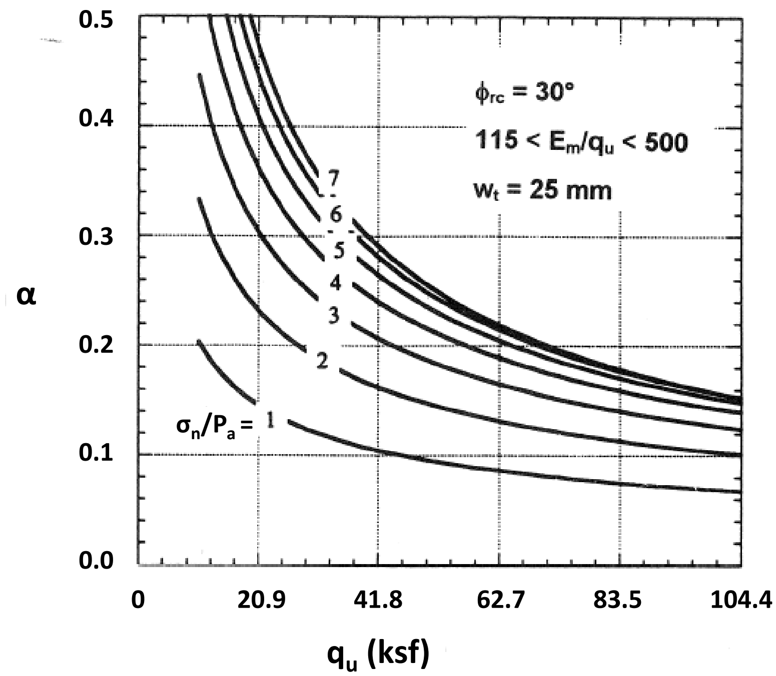

O'Neill et al. 1996

Figure 36. Factor α for cohesive IGM

The concrete pressure (σ_n) shall be calculated using the following expression:

$$\sigma_n = 0.65 \cdot \gamma_c \cdot z_i^* \tag{11}$$

where

γ_c = concrete unit weight (kcf),
z_i^* = depth below the selected cutoff elevation to the middle of a material layer i, limited to 40 ft, and
p_a = atmospheric pressure (2.12 ksf).

The correction factor (ϕ) shall be determined from Table 15 and Table 16 assuming closed joints:

Table 15. Estimation of E_m/E_i based on RQD

RQD (%)	E_m/E_i	
	Closed Joints	**Open Joints**
100	1.00	0.60
70	0.70	0.10
50	0.15	0.10
20	0.05	0.05

Source: Adapted from O'Neill and Reese 1999

Table 16. Estimation of α_E

E_m/E_i	α_E
1.0	1.0
0.5	0.8
0.3	0.7
0.1	0.55
0.05	0.45

Source: Adapted from O'Neill and Reese 1999

The resistance factor (φ_{qs}) to be applied to the nominal resistance value (q_s) shall be taken as 0.60.

The nominal unit tip resistance for shafts founded on cohesive IGM shall be computed using O'Neill and Reese (1999) as follows:

$$q_p(MPa) = 4.83[q_u(MPa)]^{0.51} \tag{12}$$

where

q_u = uniaxial compressive strength of intact rock (MPa).

The resistance factor (φ_{qp}) to be applied to the nominal resistance value shall be taken as 0.15.

5.4. Axial Resistance for Individual Drilled Shafts in Rock

The nominal unit side resistance for shaft segments located in rock shall be computed as a function of the mean uniaxial compressive strength of the intact rock according to Brown et al. (2018):

$$q_s = C \cdot p_a \cdot \left(\frac{q_u}{p_a}\right)^{0.5} < C \cdot p_a \cdot \left(\frac{f_c'}{p_a}\right)^{0.5} \tag{13}$$

where

C = 1 for "normal" rock sockets as described by Brown et al. (2018),
p_a = atmospheric pressure (2.12 ksf),
f_c' = drilled shaft 28-day concrete compressive strength in the same unit as p_a, and
q_u = uniaxial compressive strength of rock in the same unit as p_a.

The resistance factor (φ_{qs}) to be applied to the nominal resistance value (q_s) shall be taken as 0.65.

The nominal unit tip resistance for shafts founded on rock shall be computed according to Sowers (1976):

$$q_p = q_u \tag{14}$$

where

q_u = average value of the uniaxial compressive strength over a depth of 2B below the base.

The resistance factor (φ_{qp}) to be applied to the nominal resistance value (q_p) shall be taken as 0.10.

CHAPTER 6. SUMMARY AND FUTURE WORK

6.1. Summary

The design of drilled shafts in Iowa currently relies on the *AASHTO LRFD Bridge Design Specifications* (AASHTO 2017). Given that AASHTO guidelines were developed for national-level implementation, the recommended resistance factors for the design of drilled shafts may not be suitable for geological conditions and construction practices that are unique to the state of Iowa. As a result, these resistance factors may produce drilled shaft foundation designs that are overly conservative and not cost-effective. Previous research efforts led to the development of a regional database (i.e., DSHAFT) that includes load test data from Iowa and several neighboring regions. The collected data were utilized to develop regional resistance factors that have generally shown improvements over AASHTO's recommended factors (Ng. et al. 2014, Kalmogo et al. 2019).

The overall goal of this project was to provide final recommendations for the design and construction of drilled shafts in Iowa in accordance with the LRFD framework. To achieve this objective, the DSHAFT database was expanded using test data collected from Iowa, Illinois, and Nebraska, as discussed in Chapter 2. In Chapter 3, regression analyses were conducted on data from tests performed in Iowa only. These analyses investigated the correlation between soil parameters and measured unit side resistance and to develop local equations to predict resistance more accurately. In Chapter 4, production shafts in Iowa DOT bridge replacement projects were instrumented, and settlement data were collected via surveying and analyzed to gain insight on the performance of drilled shafts designed in accordance with current Iowa DOT design procedures. In Chapter 5, previous findings were utilized to develop final design recommendations; design examples illustrating implementation of the recommendations are presented in the appendix.

6.2. Recommendations for Future Research

The resistance factors recommended for implementation generally show significant improvements over those recommended by AASHTO (2017). To continuously refine the resistance factors and improve design efficiency, the following recommendations are made:

- Continuously update the regional drilled shaft test data in DSHAFT as additional data become available.
- Conduct detailed soil and rock investigations beyond the typical SPT at demonstration shaft locations.
- Verify the recommended resistance factors by performing controlled O-cell load tests in Iowa and making appropriate revisions.
- Ensure that any future load tests are conducted until large displacements are achieved or to complete geotechnical failure.
- Develop and recommend regional resistance factors for end bearing in cohesive and cohesionless soils as additional data become available.

- Using additional data from load tests performed in Iowa, conduct further regression analyses to improve correlations between soil parameters and measured resistance in order to increase the accuracy of predictions of drilled shaft capacity in Iowa geological conditions.

REFERENCES

Allen, T. M. 2005. *Development of Geotechnical Resistance Factors and Downdrag Load Factors for LRFD Foundation Strength Limit State Design*. FHWA-NHI-05-052. Federal Highway Administration, . Washington, DC.

AASHTO. 2017. *AASHTO LRFD Bridge Design Specifications*. 8th Edition. American Association of State Highway and Transportation Officials, Washington, DC.

Bowles, E. J. 1982. *Foundation Analysis and Design*. The McGraw-Hill Companies, Inc.

Brown, D. A., J. P. Turner, R. J. Castelli, and E. J. Loehr. 2018. *Drilled Shafts: Construction Procedures and Design Methods.* NHI Course No. 132014, Geotechnical Engineering Circular No. 10. National Highway Institute, Federal Highway Administration, Washington, DC.

Chen, Y.-J., and F. H. Kulhawy. 2002. Evaluation of Drained Axial Capacity for Drilled Shafts. International Deep Foundations Congress 2002, February 14–16, Orlando, FL.

Garder, J., K. W. Ng, S. Sritharan, and M. Roling. 2012. *An Electronic Database for Drilled Shaft Foundation Testing (DSHAFT)*. InTrans Project 10-366. Institute for Transportation, Ames, IA.

Iowa DOT. 2024. Section 6.3: Drilled Shafts. *Bridge Design Manual*. Iowa Department of Transportation, Ames, IA. https://iowadot.gov/bridge/policy/06-03-00DrillShaftLRFD.pdf.

Kalmogo, P., Sritharan, S., and Ashlock, J. C. 2019. *Recommended Resistance Factors for Load and Resistance Factor Design of Drilled Shafts in Iowa*. InTrans Project 14-512. Institute for Transportation, Ames, IA.

Kulhawy, F. H., S. O. Akbas, and W. A. Prakoso. 2005. Evaluation of Capacity of Rock Foundation Sockets. Alaska Rocks 2005, 40th US Symposium on Rock Mechanics, June 25–29, Anchorage, AK.

Ng, W. K., S. Sritharan, and J. C. Ashlock. 2014. *Development of Preliminary Load and Resistance Factor Design of Drilled Shafts in Iowa*. InTrans Project 11-410. Institute for Transportation, Ames, IA.

O'Neill, M. W., and L. C. Reese. 1999. *Drilled Shafts: Construction Procedures and Design Methods.* Publication No. FHWA-IF-99-025. Federal Highway Administration, Washington, DC.

O'Neill, M. W., F. C. Townsend, K. H. Hassan, A. Buller, and P. S. Chan. 1996. *Load Transfer for Drilled Shafts in Intermediate Geomaterials*. Publication No. FHWA-RD-95-171. Federal Highway Administration, McClean, VA.

Sowers, G. F. 1976. Foundation Bearing in Weathered Rock. *Rock Engineering for Foundations and Slopes*. ASCE, New York, NY, pp. 32-42.

Stark, T. D., J. H. Long, A. Osouli, and A. K. Baghdady. 2017. *Modified Standard Penetration Test–Based Drilled Shaft Design Method for Weak Rocks (Phase 2 Study)*. FHWA-ICT-17-018. Illinois Center for Transportation, Rantoul, IL.

APPENDIX: DESIGN EXAMPLES

Example 1

Drilled Shaft Design Based on Friction in Rock Socket Only. Project: TS1–US 275 over Mosquito Creek, Pottawattamie County, IA (LT-1167)

General design steps to be modified for project conditions

Design Steps	
Step 1	Develop bridge situation plan (or type, size, and location [TS&L])
Step 2	Develop soils package, including soil borings and foundation recommendations
Step 3	Determine shaft layout, shaft loads, and other design requirements
Step 4	Estimate nominal geotechnical resistance for friction and end bearing
Step 5	Select resistance factor(s) and factored resistance of each soil layer
Step 6	Estimate contract shaft length, L
Step 7	Check shaft structural capacity
Step 8	Prepare CADD notes for bridge plans.
Step 9	Check the design

Step 1. Develop bridge situation plan (or type, size, and location [TS&L])

For a typical bridge, the preliminary design engineer plots topographical information, locates the bridge, and determines the general type of superstructure, the locations of substructure units, the elevations of the foundations, hydraulic information (if needed), and other basic information to characterize the bridge. The preliminary design engineer then prepares a TS&L sheet that shows a plan and longitudinal section of the bridge.

Step 2. Develop soils package, including soil borings and foundation recommendations

Based on the location of the abutments, the soils design engineer orders soil borings, typically at least one per substructure unit. When the engineer receives the boring logs, he/she arranges for them to be plotted on a longitudinal section, checks any special geotechnical conditions on the site, and writes a recommendation for foundation type with any applicable special design considerations.

For this example, the soil profile includes the soil boring shown in Figure 37. As shown, the soil is composed of 12 ft of fat clay, 3 ft of lean to fat clay, 7 ft of lean clay, 5.5 ft of fat clay, 52.5 ft of fine sand, 5 ft of fine to coarse sand, 1.5 ft of sand with boulders, 16 ft of limestone, and 12.5 ft of weathered shale. Layer 1 is subdivided into two layers to reflect the location of the ground water table, and Layer 5 is subdivided into four layers to account for variation in the blow count number.

Step 3. Determine shaft layout, shaft loads, and other design requirements

For this example, the total factored axial compressive load supported by the foundation is assumed to be P_u = 2,500 kips. It is also assumed that there is no other type of load such as uplift or downdrag.

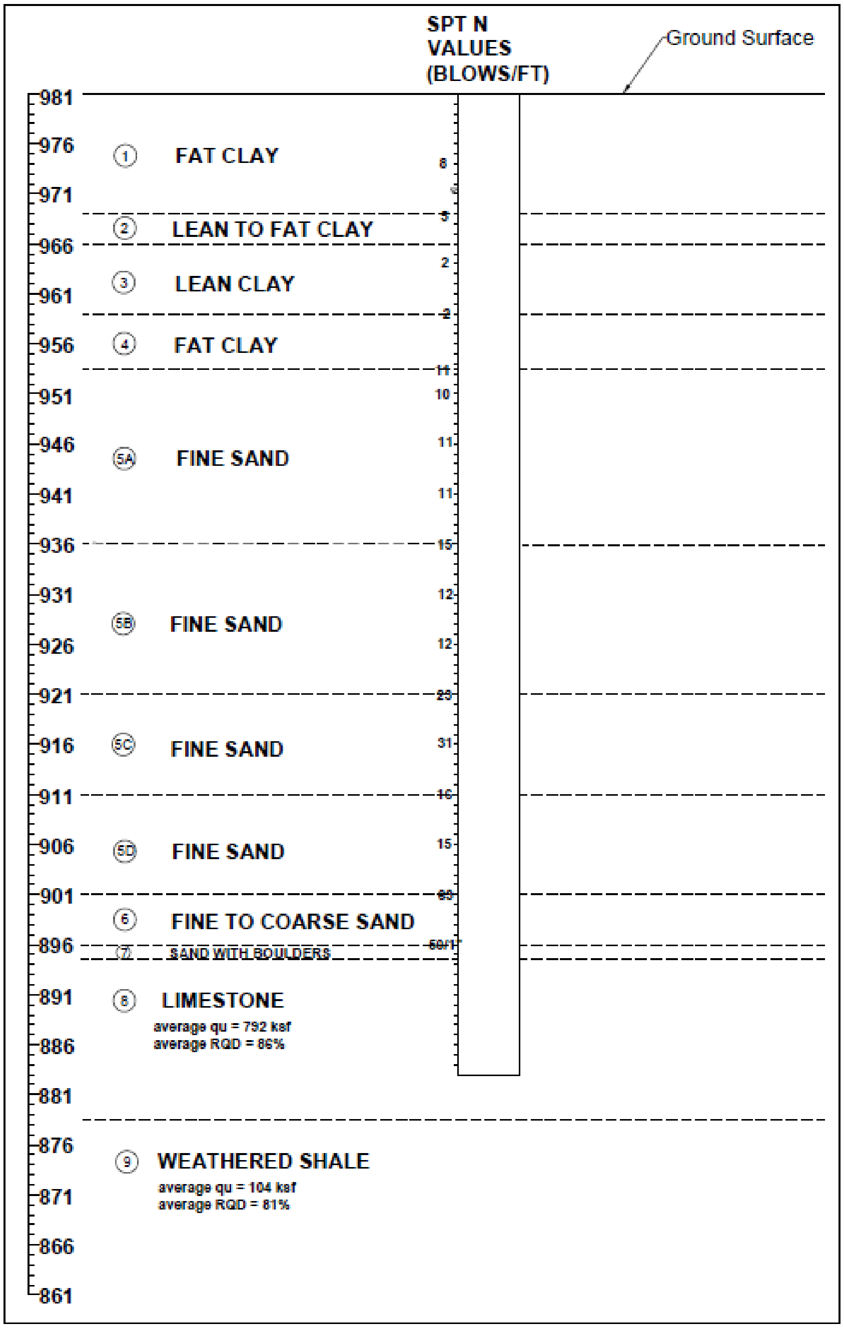

Figure 37. Example 1 soil profile

Step 4. Estimate nominal geotechnical resistance

Based on the soil boring and the recommendations in Chapter 5, the design engineer estimates the nominal unit resistances for friction bearing for each layer, as shown in Table 17 through Table 19.

Table 17. Cohesive soil layers nominal resistance

Soil Layer	Thickness Δh (ft)	SPT N Value	Unit Weight, γ (kcf)	Undrained Shear Strength, S_u (ksf)	α	q_s (ksf)
1A	5	8	0.116	1	0	0
1B	5	8	0.116	1	0.55	0.55
1C	2	8	0.120	1	0.55	0.55
2	3	5	0.115	0.625	0.55	0.34
3	7	2	0.110	0.25	0.55	0.14
4	5.5	2	0.110	0.25	0.55	0.14

Table 18. Cohesionless soil/IGM layers nominal resistance

Soil Layer	Thickness Δh (ft)	SPT N Value	Unit Weight, γ (kcf)	z (ft)	β	σ_v' (ksf)	q_s (ksf)
5A	17.5	11	0.118	36.25	0.49	2.52	1.21
5B	15	13	0.120	52.5	0.45	3.43	1.48
5C	10	27	0.123	65	0.41	4.17	1.63
5D	10	16	0.111	75	0.33	4.72	1.51
6	5	63	0.137	82.5	0.27	5.15	1.37
7	1.5	refusal (limit to 100)	0.140	85.75	0.25	5.39	1.32

Table 19. Rock nominal resistance

Soil Layer	Thickness Δh (ft)	q_u (ksf)	RQD (%)	α_E	q_s (ksf)	q_p (ksf)
8	16	792	86	1.0	41.57	279.36
9	12.5	104	81	1.0	14.85	-

Step 5. Select resistance factor and estimate factored resistance of each layer

In this step, the design engineer selects the appropriate resistance factor for each soil type. The soil profile in this example is composed of a combination of cohesive soils, cohesionless soils, cohesionless IGM, and rock. As recommended in Chapter 5, the following resistance factors are used:

φ_{qs} = 0.50 for skin friction in cohesive soil layers
φ_{qs} = 0.75 for skin friction in cohesionless soil layers
φ_{qs} = 0.75 for skin friction in cohesionless IGM layers

φ_{qs} = 0.65 for skin friction in rock
φ_{qp} = 0.10 for end bearing in rock

Table 20. Factored resistance

Soil Layer	Skin Friction			End Bearing		
	q_s (ksf)	φ_{qs}	R_{sR} (ksf)	q_p (ksf)	φ_{qp}	R_{pR} (ksf)
1A	0	0.50	0	-	-	-
1B	0.55	0.50	0.28	-	-	-
1C	0.55	0.50	0.28	-	-	-
2	0.34	0.50	0.17	-	-	-
3	0.14	0.50	0.07	-	-	-
4	0.14	0.50	0.07	-	-	-
5A	1.21	0.75	0.91	-	-	-
5B	1.48	0.75	1.11	-	-	-
5C	1.63	0.75	1.22	-	-	-
5D	1.51	0.75	1.13	-	-	-
6	1.37	0.75	1.03	-	-	-
7	1.32	0.75	0.99	-	-	-
8	41.57	0.65	27.02	279.36	0.10	27.94
9	14.85	0.65	9.65	-	-	-

Step 6. Estimate contract drilled shaft length, L, based on skin friction in rock socket only

The required shaft length is determined based solely on the factored skin resistance from the rock socket, as determined in Step 5 and presented in Table 20. For this example, a nominal shaft diameter of 6.5 ft and a rock socket diameter of 6 ft are assumed. The skin friction of the soil layers as well as the tip resistance in the rock socket are neglected. The cumulative factored geotechnical resistance, R_R, along the shaft is calculated as follows, where L is the total shaft length below the ground surface:

L_0 = 0 ft, R_{sR0} = 0
L_1 = 5 ft, $R_{sR1} = R_{sR0}$ + (0 ksf) (5 ft) (π) (6.5 ft) = 0 kips
L_2 = 5 + 5 = 10 ft, $R_{sR2} = R_{sR1}$ + (0 ksf) (5 ft) (π) (6.5 ft) = 0 + 0 = 0 kips
L_3 = 10 + 2 = 12 ft, $R_{sR3} = R_{sR2}$ + (0 ksf) (2 ft) (π) (6.5 ft) = 0 + 0 = 0 kips
L_4 = 12 + 3 = 15 ft, $R_{sR4} = R_{sR3}$ + (0 ksf) (3 ft) (π) (6.5 ft) = 0 + 0 = 0 kips
L_5 = 15 + 7 = 22 ft, $R_{sR5} = R_{sR4}$ + (0 ksf) (7 ft) (π) (6.5 ft) = 0 + 0 = 0 kips
L_6 = 22 + 5.5 = 27.5 ft, $R_{sR6} = R_{sR5}$ + (0 ksf) (5.5 ft) (π) (6.5 ft) = 0 + 0 = 0 kips
L_7 = 27.5 + 17.5 = 45 ft, $R_{sR7} = R_{sR6}$ + (0 ksf) (17.5 ft) (π) (6.5 ft) = 0 + 0 = 0 kips
L_8 = 45 + 15 = 60 ft, $R_{sR8} = R_{sR7}$ + (0 ksf) (15 ft) (π) (6.5 ft) = 0 + 0 = 0 kips
L_9 = 60 + 10 = 70 ft, $R_{sR9} = R_{sR8}$ + (0 ksf) (10 ft) (π) (6.5 ft) = 0 + 0 = 0 kips
L_{10} = 70 + 10 = 80 ft, $R_{sR10} = R_{sR9}$ + (0 ksf) (10 ft) (π) (6.5 ft) = 0 + 0 = 0 kips
L_{11} = 80 + 5 = 85 ft, $R_{sR11} = R_{sR10}$ + (0 ksf) (5 ft) (π) (6.5 ft) = 0 + 0 = 0 kips
L_{12} = 85 + 1.5 = 86.5 ft, $R_{sR12} = R_{sR11}$ + (0 ksf) (1.5 ft) (π) (6 ft) = 0 + 0 = 0 kips
L_{13} = 86.5 + 6 = 92.5 ft, $R_{sR13} = R_{sR12}$ + (27.02 ksf) (6 ft) (π) (6 ft) = 0 + 3,055.95 = 3,055.95 kips

The estimated nominal geotechnical resistance versus depth is presented in Figure 38.

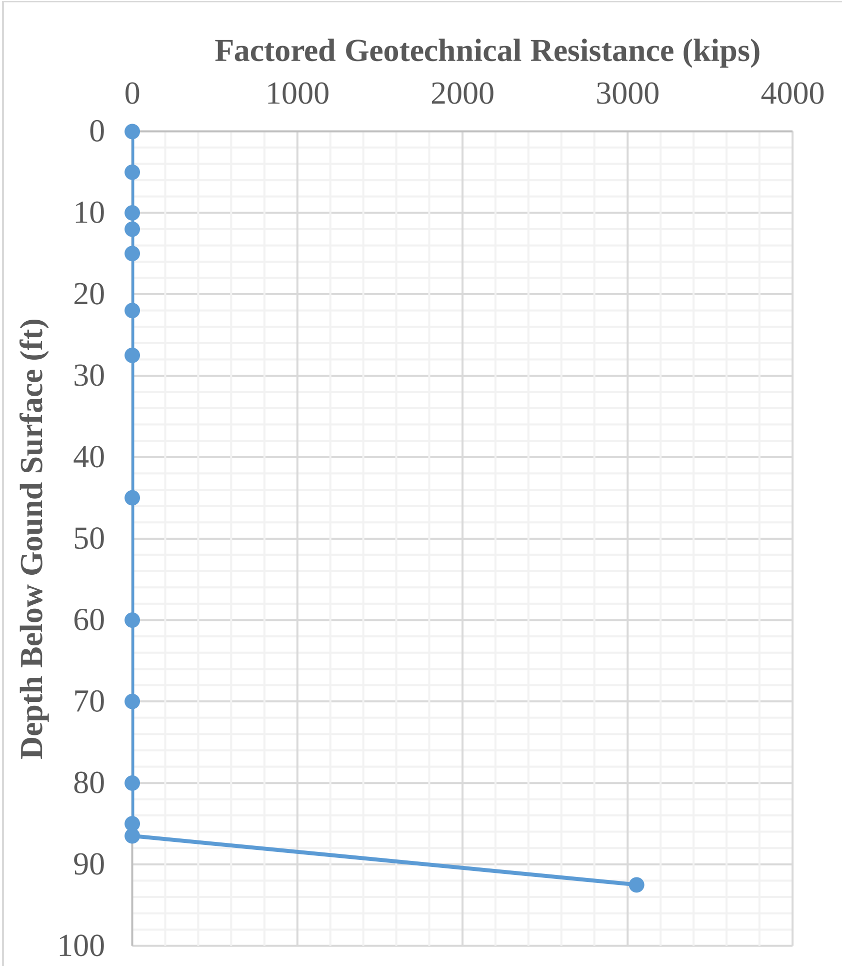

Figure 38. Example 1 plot of nominal geotechnical resistance versus depth

Based on load test data, the measured skin friction in the rock socket at 1 in. top displacement is 11,279 kips, which is well above the predicted factored resistance of 3,055.95 kips. A contract shaft length of 92.5 ft is adequate to support the required load of 2,500 kips. There is no need to consider the skin friction from other soil layers or the end bearing in the rock socket. However, doing so could lead to reduced shaft dimensions and reduced project costs.

Step 7. Check shaft structural capacity

The shaft reinforcement details shall be selected and appropriate checks shall be made to ensure that the design load does not compromise the structural integrity of the shaft.

Step 8. Prepare CADD notes for bridge plans

Step 9. Check the design

Example 2

Drilled Shaft Design Based on Friction and End Bearing in Rock Socket and Friction in All Other Soil Layers. Project: TS1–US 275 over Mosquito Creek, Pottawattamie County, IA (LT-1167)

General design steps to be modified for project conditions

Design Steps	
Step 1	Develop bridge situation plan (or type, size, and location [TS&L])
Step 2	Develop soils package, including soil borings and foundation recommendations
Step 3	Determine shaft layout, shaft loads, and other design requirements
Step 4	Estimate nominal geotechnical resistance for friction and end bearing
Step 5	Select resistance factor(s) and factored resistance of each soil layer
Step 6	Estimate contract shaft length, L
Step 7	Check shaft structural capacity
Step 8	Prepare CADD notes for bridge plans
Step 9	Check the design

Step 1. Develop bridge situation plan (or type, size, and location [TS&L])

For a typical bridge, the preliminary design engineer plots topographical information, locates the bridge, and determines the general type of superstructure, the locations of substructure units, the elevations of the foundations, hydraulic information (if needed), and other basic information to characterize the bridge. The preliminary design engineer then prepares a TS&L sheet that shows a plan and longitudinal section of the bridge.

Step 2. Develop soils package, including soil borings and foundation recommendations

Based on the location of the abutments, the soils design engineer orders soil borings, typically at least one per substructure unit. When the engineer receives the boring logs, he/she arranges for them to be plotted on a longitudinal section, checks any special geotechnical conditions on the site, and writes a recommendation for foundation type with any applicable special design considerations.

For this example the soil profile include the soil boring shown in Figure 39. As shown, the soil is composed of 12 ft of fat clay, 3 ft of lean to fat clay, 7 ft of lean clay, 5.5 ft of fat clay, 52.5 ft of fine sand, 5 ft of fine to coarse sand, 1.5 ft of sand with boulders, 16 ft of limestone, and 12.5 ft of weathered shale. Layer 1 is subdivided into two layers to reflect the location of the ground water table, and Layer 5 is subdivided into four layers to account for variation in the blow count number.

Step 3. Determine shaft layout, shaft loads, and other design requirements

For this example, the total factored axial compressive load supported by the foundation is assumed to be P_u = 2,500 kips. It is also assumed that there is no other type of load such as uplift or downdrag.

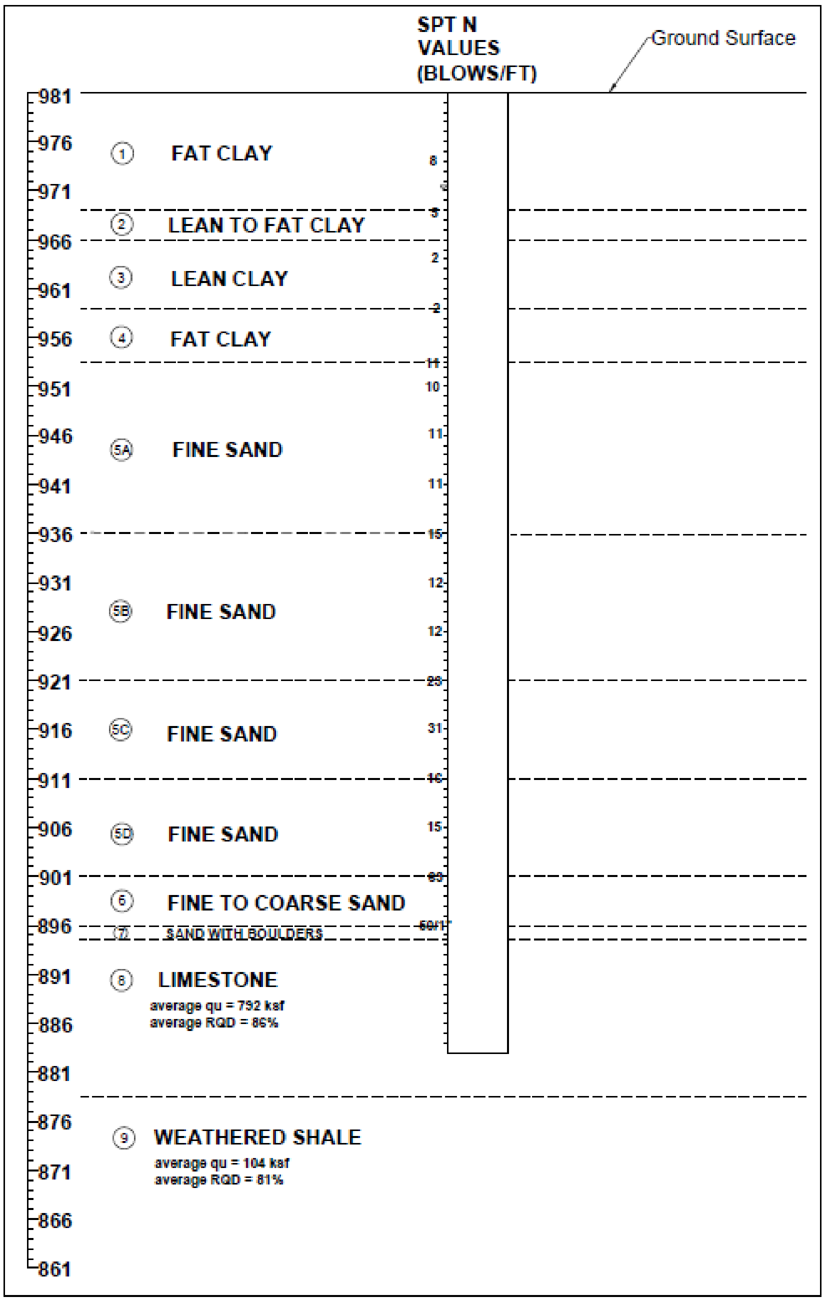

Figure 39. Example 2 soil profile

Step 4. Estimate nominal geotechnical resistance

Based on the soil boring and the recommendations in Chapter 5, the design engineer estimates the nominal unit resistances for friction bearing for each layer, as shown in Table 21, Table 22, and Table 23.

Table 21. Cohesive soil layers nominal resistance

Soil Layer	Thickness Δh (ft)	SPT N Value	Unit Weight, γ (kcf)	Undrained Shear Strength, S_u (ksf)	α	q_s (ksf)
1A	5	8	0.116	1	0	0
1B	5	8	0.116	1	0.55	0.55
1C	2	8	0.120	1	0.55	0.55
2	3	5	0.115	0.625	0.55	0.34
3	7	2	0.110	0.25	0.55	0.14
4	5.5	2	0.110	0.25	0.55	0.14

Table 22. Cohesionless soil/IGM layers nominal resistance

Soil Layer	Thickness Δh (ft)	SPT N Value	Unit Weight, γ (kcf)	z (ft)	β	σ_v' (ksf)	q_s (ksf)
5A	17.5	11	0.118	36.25	0.49	2.52	1.21
5B	15	13	0.120	52.5	0.45	3.43	1.48
5C	10	27	0.123	65	0.41	4.17	1.63
5D	10	16	0.111	75	0.33	4.72	1.51
6	5	63	0.137	82.5	0.27	5.15	1.37
7	1.5	refusal (limit to 100)	0.140	85.75	0.25	5.39	1.32

Table 23. Rock nominal resistance

Soil Layer	Thickness Δh (ft)	q_u (ksf)	RQD (%)	α_E	q_s (ksf)	q_p (ksf)
8	16	792	86	1.0	41.57	279.36
9	12.5	104	81	1.0	14.85	-

Step 5. Select resistance factor and estimate factored resistance of each layer

In this step, the design engineer selects the appropriate resistance factor for each soil type. The soil profile in this example is composed of a combination of cohesive soils, cohesionless soils, cohesionless IGM, and rock. As recommended in Chapter 5, the following resistance factors are used:

φ_{qs} = 0.50 for skin friction in cohesive soil layers
φ_{qs} = 0.75 for skin friction in cohesionless soil layers
φ_{qs} = 0.75 for skin friction in cohesionless IGM layers

φ_{qs} = 0.65 for skin friction in rock
φ_{qp} = 0.10 for end bearing in rock

Table 24. Factored resistance

Soil Layer	Skin Friction			End Bearing		
	q_s (ksf)	φ_{qs}	R_{sR} (ksf)	q_p (ksf)	φ_{qp}	R_{pR} (ksf)
1A	0	0.50	0	-	-	-
1B	0.55	0.50	0.28	-	-	-
1C	0.55	0.50	0.28	-	-	-
2	0.34	0.50	0.17	-	-	-
3	0.14	0.50	0.07	-	-	-
4	0.14	0.50	0.07	-	-	-
5A	1.21	0.75	0.91	-	-	-
5B	1.48	0.75	1.11	-	-	-
5C	1.63	0.75	1.22	-	-	-
5D	1.51	0.75	1.13	-	-	-
6	1.37	0.75	1.03	-	-	-
7	1.32	0.75	0.99	-	-	-
8	41.57	0.65	27.02	279.36	0.10	27.94
9	14.85	0.65	9.65			

Step 6. Estimate contract drilled shaft length, L, based on skin friction and end bearing in rock socket and skin friction in overlying soil layers

The required shaft length is determined considering the factored resistance from all sources, including skin friction in all soils, skin friction in the rock socket, and end bearing in the rock socket. The factored resistances were determined in Step 5 and are presented in Table 24. For this example, a nominal shaft diameter of 6.5 ft and a rock socket diameter of 6 ft are assumed. The cumulative factored geotechnical resistance, R_R, along the shaft is calculated as follows, where L is the total shaft length below the ground surface:

L_0 = 0 ft, R_{sR0} = 0
L_1 = 5 ft, R_{sR1} = R_{sR0} + (0 ksf) (5 ft) (π) (6.5 ft) = 0 kips
L_2 = 5 + 5 = 10 ft, R_{sR2} = R_{sR1} + (0.29 ksf) (5 ft) (π) (6.5 ft) = 0 + 28.08 = 28.08 kips
L_3 = 10 + 2 = 12 ft, R_{sR3} = R_{sR2} + (0.29 ksf) (2 ft) (π) (6.5 ft) = 28.08+ 11.23 = 39.31 kips
L_4 = 12 + 3 = 15 ft, R_{sR4} = R_{sR3} + (0.18 ksf) (3 ft) (π) (6.5 ft) = 39.31 + 10.41 = 49.72 kips
L_5 = 15 + 7 = 22 ft, R_{sR5} = R_{sR4} + (0.07 ksf) (7 ft) (π) (6.5 ft) = 49.72 + 10.01 = 59.73 kips
L_6 = 22 + 5.5 = 27.5 ft, R_{sR6} = R_{sR5} + (0.07 ksf) (5.5 ft) (π) (6.5 ft) = 59.73 + 7.86 = 67.59 kips
L_7 = 27.5 + 17.5 = 45 ft, R_{sR7} = R_{sR6} + (0.91 ksf) (17.5 ft) (π) (6.5 ft) = 67.59 + 325.19 = 392.78 kips
L_8 = 45 + 15 = 60 ft, R_{sR8} = R_{sR7} + (1.11 ksf) (15 ft) (π) (6.5 ft) = 392.78+ 400.00 = 792.78 kips
L_9 = 60 + 10 = 70 ft, R_{sR9} = R_{sR8} + (1.22 ksf) (10 ft) (π) (6.5 ft) = 792.78 + 249.13 = 1,041.91 kips
L_{10} = 70 + 10 = 80 ft, R_{sR10} = R_{sR9} + (1.13 ksf) (10 ft) (π) (6.5 ft) = 1,041.91 + 230.75 = 1,272.66 kips

L_{11} = 80 + 5 = 85 ft, $R_{sR11} = R_{sR10}$ + (1.03 ksf) (5 ft) (π) (6.5 ft) = 1,272.66 + 105.16 = 1,377.82 kips

L_{12} = 85 + 1.5 = 86.5 ft, $R_{sR12} = R_{sR11}$ + (0.99 ksf) (1.5 ft) (π) (6 ft) = 1,377.82 + 27.99 = 1,405.81 kips

L_{13} = 86.5 + 6 = 92.5 ft, $R_{sR13} = R_{sR12}$ + (27.02 ksf) (6 ft) (π) (6 ft) + (27.94 ksf) (π) $\frac{(6\text{ ft})^2}{4}$= 1,405.81 + 3,055.95 + 789.87 = 5,251.63 kips

The estimated nominal geotechnical resistance versus depth is presented in Figure 40.

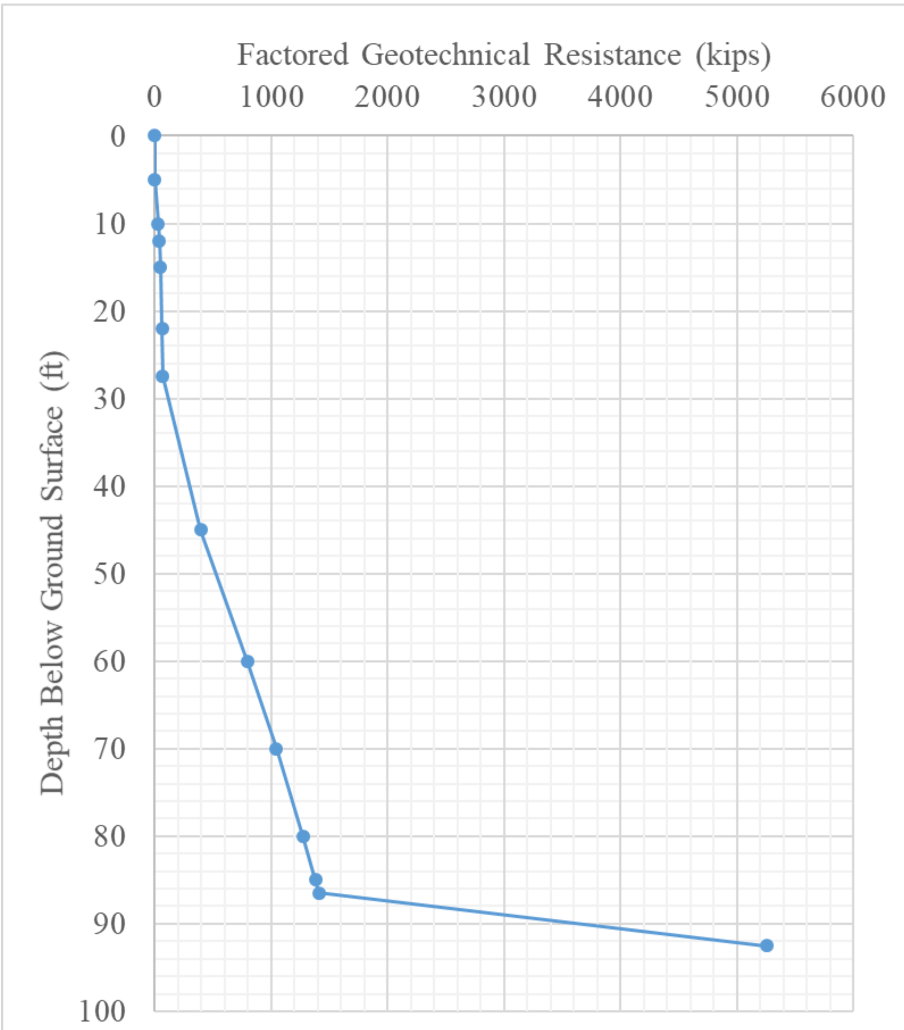

Figure 40. Example 2 plot of nominal geotechnical resistance versus depth

Based on load test data, the measured total load at 1 in. top displacement is 19,013 kips, which is well above the predicted factored resistance of 5,252 kips. A contract shaft length of 92.5 ft, as recommended for this particular project, can be used to support the required load of 2,500 kips. As observed, significant additional resistance can be obtained from the soil layers overlying the bedrock and from the end bearing. In this example, the factored geotechnical resistance is 2.06

times the design load. The shaft diameter can be decreased and still meet the design requirements, thus reducing the overall project cost.

Step 7. Check shaft structural capacity

Step 8. Prepare CAD notes for bridge plans

Step 9. Check the design

Example 3

Drilled Shaft Design Based on Friction in Rock Socket Only. Project: TS1–I-29 over Mosquito Creek, Pottawattamie County, IA (LT-1128)

General design steps to be modified for project conditions

Design Steps	
Step 1	Develop bridge situation plan (or type, size, and location [TS&L])
Step 2	Develop soils package, including soil borings and foundation recommendations
Step 3	Determine shaft layout, shaft loads, and other design requirements
Step 4	Estimate nominal geotechnical resistance for friction and end bearing
Step 5	Select resistance factor(s) and factored resistance of each soil layer
Step 6	Estimate contract shaft length, L
Step 7	Check shaft structural capacity
Step 8	Prepare CADD notes for bridge plans.
Step 9	Check the design

Step 1. Develop bridge situation plan (or type, size, and location [TS&L])

For a typical bridge, the preliminary design engineer plots topographical information, locates the bridge, and determines the general type of superstructure, the locations of substructure units, the elevations of the foundations, hydraulic information (if needed), and other basic information to characterize the bridge. The preliminary design engineer then prepares a TS&L sheet that shows a plan and longitudinal section of the bridge.

Step 2. Develop soils package, including soil borings and foundation recommendations

Based on the location of the abutments, the soils design engineer orders soil borings, typically at least one per substructure unit. When the engineer receives the boring logs, he/she arranges for them to be plotted on a longitudinal section, checks any special geotechnical conditions on the site, and writes a recommendation for foundation type with any applicable special design considerations.

For this example, the soil profile includes the soil boring shown in Figure 41. As shown, the soil is composed of 28 ft of fat clay, 15 ft of silty fine sand, 25 ft of fine sand, 5 ft of fine to medium sand, 5 ft of silty fine sand, 8 ft of fine to medium sand, 3.5 ft of highly weathered shale, 7.2 of moderately weathered to highly weathered shale, 15 ft of slightly weathered limestone, and 6 ft of moderately weathered to highly weathered shale.

Step 3. Determine shaft layout, shaft loads, and other design requirements

For this example, the total factored axial compressive load supported by the foundation is assumed to be P_u = 2,069 kips. It is also assumed that there is no other type of load such as uplift or downdrag.

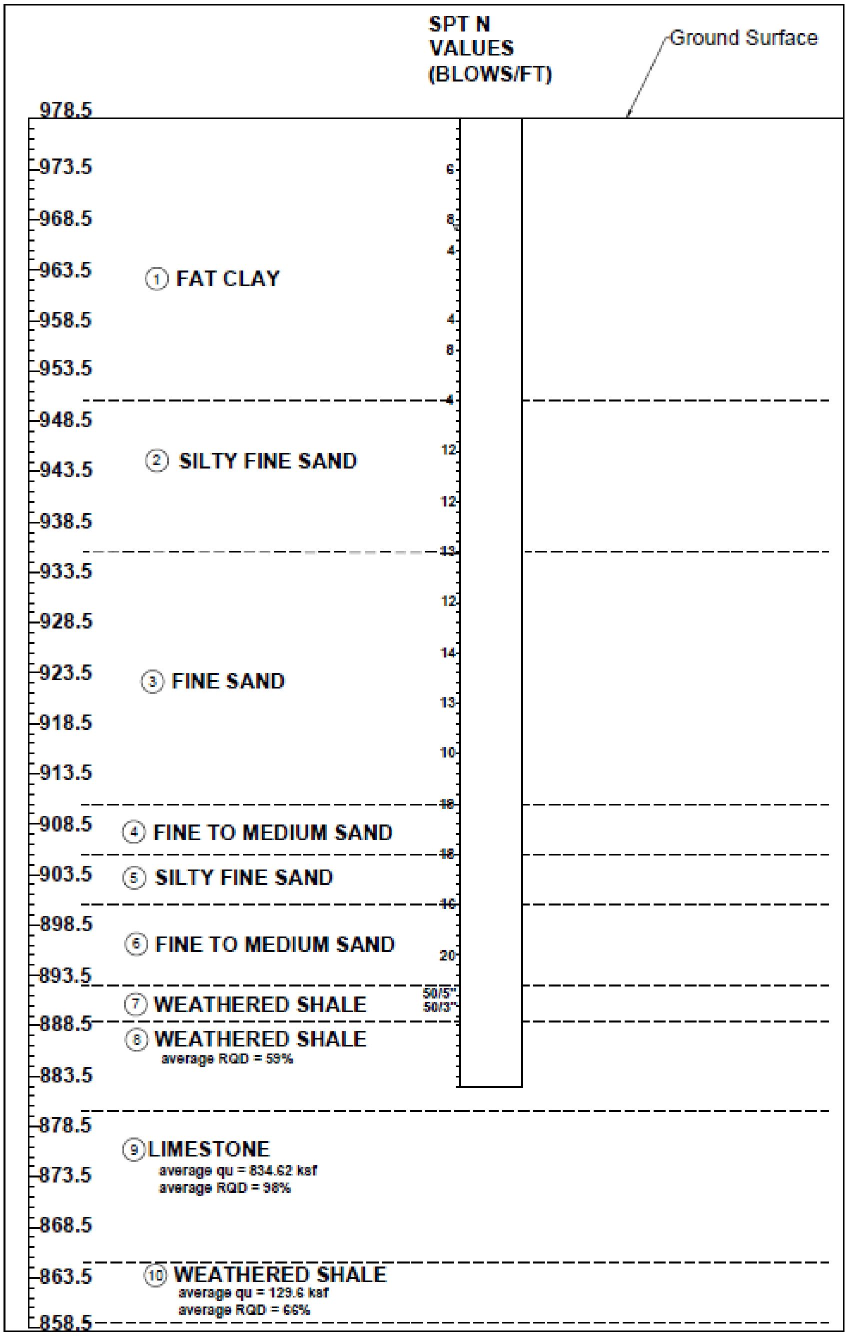

Figure 41. Example 3 soil profile

Step 4. Estimate nominal geotechnical resistance for friction

Based on the soil boring and the recommendations in Chapter 5, the design engineer estimates the nominal unit resistances for friction bearing for each layer, as shown in Table 25 through Table 27.

Table 25. Cohesive soil layers nominal resistance

Soil Layer	Thickness Δh (ft)	SPT N Value	Unit Weight, γ (kcf)	Undrained Shear Strength, S_u (ksf)	α	q_s (ksf)
1A	5	6	0.125	0.75	0	0
1B	6	6	0.125	0.75	0.55	0.41
1C	17	6	0.113	0.75	0.55	0.41
7	3.5	refusal	0.140	4.99	0.46	2.32

Table 26. Cohesionless soil layers nominal resistance

Soil Layer	Thickness Δh (ft)	SPT N Value	Unit Weight, γ (kcf)	z (ft)	β	σ_v' (ksf)	q_s (ksf)
2	15	9	0.111	35.5	0.43	2.73	1.01
3	25	12	0.112	55.5	0.41	3.77	1.56
4	5	19	0.119	70.5	0.37	4.59	1.09
5	5	18	0.118	75.5	0.33	4.90	1.55
6	8	18	0.118	82	0.28	5.29	1.42

Table 27. Rock nominal resistance

Soil Layer	Thickness Δh (ft)	q_u (ksf)	RQD (%)	q_s (ksf)	q_p (ksf)
8	9.1	129.6	59	16.58	895.2

Note: Since no other measured values were available, q_u is assumed to be the same as that of layer 10.

Step 5. Select resistance factor and estimate factored resistance of each layer

In this step, the design engineer selects the appropriate resistance factor for each soil type. The soil profile in this example is composed of a combination of cohesive soils, cohesionless soils, cohesionless IGM, and rock. As recommended in Chapter 5, the following resistance factors are used:

φ_{qs} = 0.50 for skin friction in cohesive soil layers
φ_{qs} = 0.75 for skin friction in cohesionless soil layers
φ_{qs} = 0.75 for skin friction in cohesionless IGM layers
φ_{qs} = 0.65 for skin friction in rock
φ_{qp} = 0.10 for end bearing in rock

Table 28. Factored geotechnical side resistance

Soil Layer	Skin Friction			End Bearing		
	q_s (ksf)	φ_{qs}	R_{sR} (ksf)	q_p (ksf)	φ_{qp}	R_{pR} (ksf)
1A	0	0.50	0	-	-	-
1B	0.41	0.50	0.21	-	-	-
2	0.41	0.50	0.21	-	-	-
3	1.01	0.75	0.76	-	-	-
4	1.56	0.75	1.17	-	-	-
5	1.09	0.75	0.82	-	-	-
6	1.55	0.75	1.16	-	-	-
7	1.42	0.75	1.06	-	-	-
8	2.32	0.50	1.16	895.2	0.10	89.52
9	16.58	0.65	10.78	-	-	-

Step 6. Estimate contract drilled shaft length, L, based on skin friction in rock socket only

The required shaft length is determined based solely on the factored skin resistance from the rock socket, as determined in Step 5 and presented in Table 28. For this example, a nominal shaft diameter of 6 ft and a rock socket diameter of 5.5 ft are assumed. The skin friction of the soil layers as well as the tip resistance in the rock socket are neglected. The cumulative factored geotechnical resistance, R_R, along the shaft is calculated as follows, where L is the total shaft length below the ground surface:

L_0 = 0 ft, R_{sR0} = 0
L_1 = 5 ft, $R_{sR1} = R_{sR0}$ + (0 ksf) (5 ft) (π) (6 ft) = 0 kips
L_2 = 5 + 6 = 11 ft, $R_{sR2} = R_{sR1}$ + (0 ksf) (0.21 ft) (π) (6 ft) = 0 + 0 = 0 kips
L_3 = 11 + 17 = 28 ft, $R_{sR3} = R_{sR2}$ + (0 ksf) (17 ft) (π) (6 ft) = 0 + 0 = 0 kips
L_4 = 28 + 15 = 43 ft, $R_{sR4} = R_{sR3}$ + (0 ksf) (15 ft) (π) (6 ft) = 0 + 0 = 0 kips
L_5 = 43 + 25 = 68 ft, $R_{sR5} = R_{sR4}$ + (0 ksf) (25 ft) (π) (6 ft) = 0 + 0 = 0 kips
L_6 = 68 + 5 = 73 ft, $R_{sR6} = R_{sR5}$ + (0 ksf) (5 ft) (π) (6 ft) = 0 + 0 = 0 kips
L_7 = 73 + 5 = 78 ft, $R_{sR7} = R_{sR6}$ + (0 ksf) (5 ft) (π) (6 ft) = 0 + 0 = 0 kips
L_8 = 78 + 8 = 86 ft, $R_{sR8} = R_{sR7}$ + (0 ksf) (8 ft) (π) (6 ft) = 0 + 0 = 0 kips
L_9 = 86 + 3.5 = 89.5 ft, $R_{sR9} = R_{sR8}$ + (0 ksf) (3.5 ft) (π) (5.5 ft) = 0 + 0 = 0 kips
L_{10} = 89.5 + 7 = 96.5 ft, $R_{sR10} = R_{sR9}$ + (10.78 ksf) (9 ft) (π) (5.5 ft) = 0 + 1,322.11 = 1,322.11 kips

The estimated nominal geotechnical resistance versus depth is presented in Figure 42.

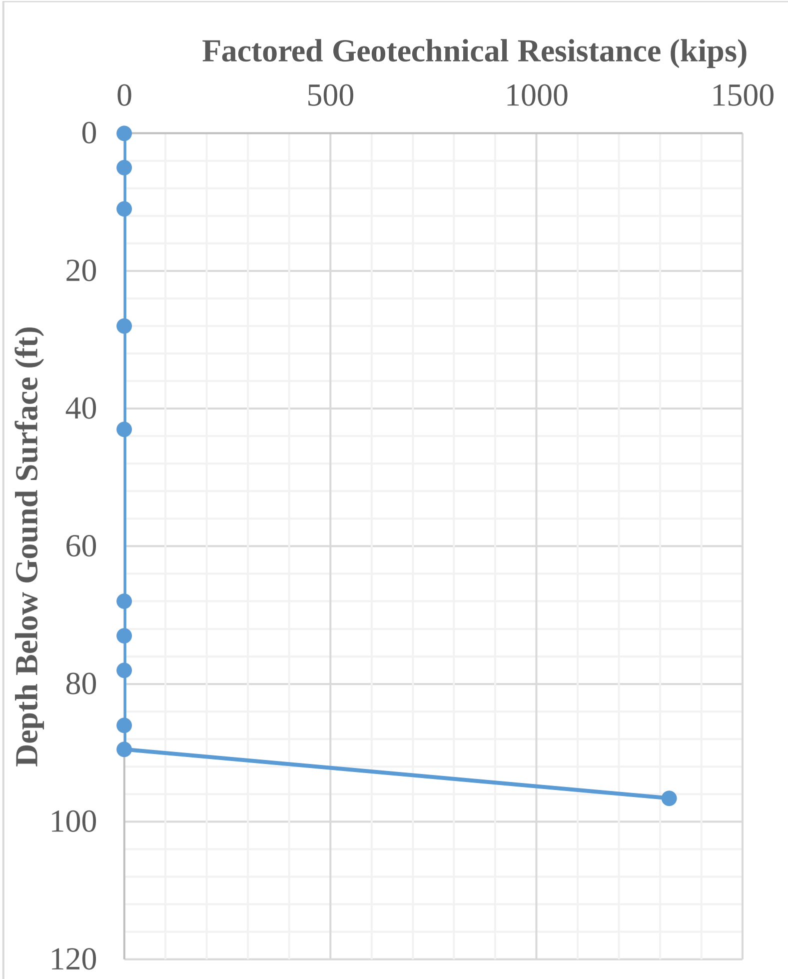

Figure 42. Example 3 plot of nominal geotechnical resistance versus depth

Based on load test data, the measured skin friction in the rock socket at 1 in. top displacement is 2,452 kips for the contract length of 96.5 ft. The predicted factored resistance for the same contract length is 1,322 kips, which is less than the design load of 2,069 kips. If no load test had been performed, the rock socket would have had to be extended into the limestone layer to increase the skin friction and meet the design requirements, resulting in an increase in project costs. Alternatively, the designer can account for the skin friction from the soil layers overlying the bedrock as well as from the end bearing and verify that the predicted factored resistance is greater than or equal to the design load.

Step 7. Estimate contract drilled shaft length, L, based on skin friction and end bearing in rock socket and skin friction in overlying soil layers

The required shaft length is determined considering the factored resistance from all sources, including skin friction in all soils, skin friction in the rock socket, and end bearing in the rock socket. The factored resistances were determined in Step 5 and are presented in Table 28. The cumulative factored geotechnical resistance, R_R, along the shaft is calculated as follows, where L is the total shaft length below the ground surface:

L_0 = 0 ft, R_{sR0} = 0
L_1 = 5 ft, $R_{sR1} = R_{sR0}$ + (0 ksf) (5 ft) (π) (6 ft) = 0 kips
L_2 = 5 + 6 = 11 ft, $R_{sR2} = R_{sR1}$ + (0.21 ksf) (0.21 ft) (π) (6 ft) = 0 +23.18 = 23.18 kips
L_3 = 11 + 17 = 28 ft, $R_{sR3} = R_{sR2}$ + (0.21 ksf) (17 ft) (π) (6 ft) = 23.18 + 65.69 = 88.88 kips
L_4 = 28 + 15 = 43 ft, $R_{sR4} = R_{sR3}$ + (0.76 ksf) (15 ft) (π) (6 ft) = 88.88 + 214.88 = 303.76 kips
L_5 = 43 + 25 = 68 ft, $R_{sR5} = R_{sR4}$ + (1.17 ksf) (25 ft) (π) (6 ft) = 303.76 + 551.35 = 855.11 kips
L_6 = 68 + 5 = 73 ft, $R_{sR6} = R_{sR5}$ + (0.82 ksf) (5 ft) (π) (6 ft) = 855.11 + 77.28 = 932.39 kips
L_7 = 73 + 5 = 78 ft, $R_{sR7} = R_{sR6}$ + (1.16 ksf) (5 ft) (π) (6 ft) = 932.39 + 109.33= 1,041.72 kips
L_8 = 78 + 8 = 86 ft, $R_{sR8} = R_{sR7}$ + (1.06 ksf) (8 ft) (π) (6 ft) = 1,041.72 + 159.84 = 1,201.56 kips
L_9 = 86 + 3.5 = 89.5 ft, $R_{sR9} = R_{sR8}$ + (1.16 ksf) (3.5 ft) (π) (5.5 ft) = 1,201.56 + 70.15= 1,271.71 kips
L_{10} = 89.5 + 7 = 96.5 ft, $R_{sR10} = R_{sR9}$ + (10.94 ksf) (6.75 ft) (π) (5.5 ft) + (89.52 ksf) (π) $\frac{(5.5\text{ ft})^2}{4}$ = 1,271.71 + 1,256.94 + 2,126.84 = 4,655.49 kips

The estimated nominal geotechnical resistance versus depth is presented in Figure 43.

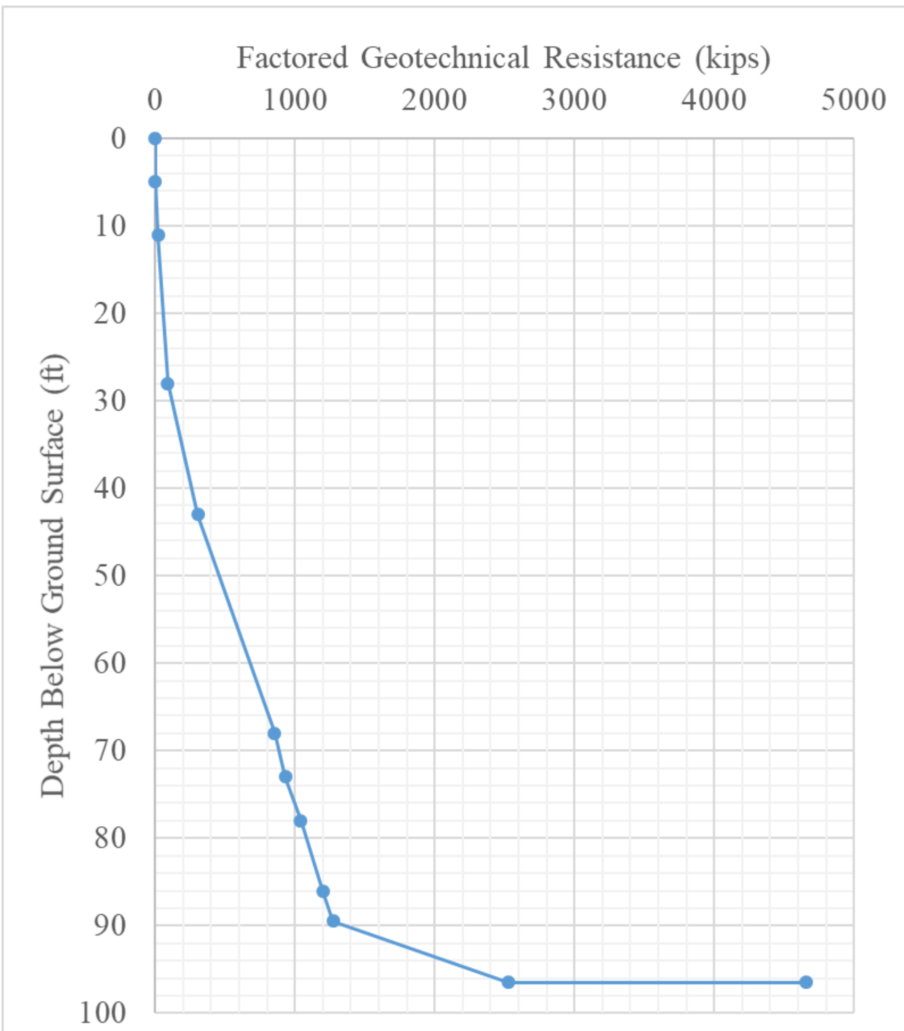

Figure 43. Example 3 plot of nominal geotechnical resistance versus depth

Based on load test data, the measured total load at 1 in. top displacement is 9,105 kips, which is well above the predicted factored resistance of 4,655 kips. If the end bearing in the bedrock and the skin friction from the soil layers are considered, the contract shaft length of 96.5 ft, which was previously found to be inadequate, can be used to support the required load of 2,069 kips. The shaft diameter could even be reduced, since the factored geotechnical resistance was found to be more than two times the design load.

Step 8. Check shaft structural capacity

The shaft reinforcement details shall be selected and appropriate checks shall be made to ensure that the design load does not compromise the structural integrity of the shaft.

Step 9. Prepare CADD notes for bridge plans

Step 10. Check the design

Example 4

Drilled Shaft Design Based on Friction in Soil. Project: TS1 –US 52/IA 64 over Mississippi River, Jackson County, IA (LT-1794-1)

General design steps to be modified for project conditions

Design Steps	
Step 1	Develop bridge situation plan (or type, size, and location [TS&L])
Step 2	Develop soils package, including soil borings and foundation recommendations
Step 3	Determine shaft layout, shaft loads, and other design requirements
Step 4	Estimate nominal geotechnical resistance for friction and end bearing
Step 5	Select resistance factor(s) and factored resistance of each soil layer
Step 6	Estimate contract shaft length, L
Step 7	Check shaft structural capacity
Step 8	Prepare CADD notes for bridge plans.
Step 9	Check the design

Step 1. Develop bridge situation plan (or type, size, and location [TS&L])

For a typical bridge, the preliminary design engineer plots topographical information, locates the bridge, and determines the general type of superstructure, the locations of substructure units, the elevations of the foundations, hydraulic information (if needed), and other basic information to characterize the bridge. The preliminary design engineer then prepares a TS&L sheet that shows a plan and longitudinal section of the bridge.

Step 2. Develop soils package, including soil borings and foundation recommendations

Based on the location of the abutments, the soils design engineer orders soil borings, typically at least one per substructure unit. When the engineer receives the boring logs, he/she arranges for them to be plotted on a longitudinal section, checks any special geotechnical conditions on the site, and writes a recommendation for foundation type with any applicable special design considerations.

For this example, the soil profile includes the soil boring shown in Figure 44. As shown, the soil is predominantly composed of poorly graded sand overlain by a 4 ft layer of silty clay. The poorly graded sand is subdivided into several different layers to account for variation in the blow count number.

Step 3. Determine shaft layout, shaft loads, and other design requirements

For this example, the total factored axial compressive load supported by the foundation is assumed to be $P_u = 1,500$ kips. It is also assumed that there is no other type of load such as uplift or downdrag.

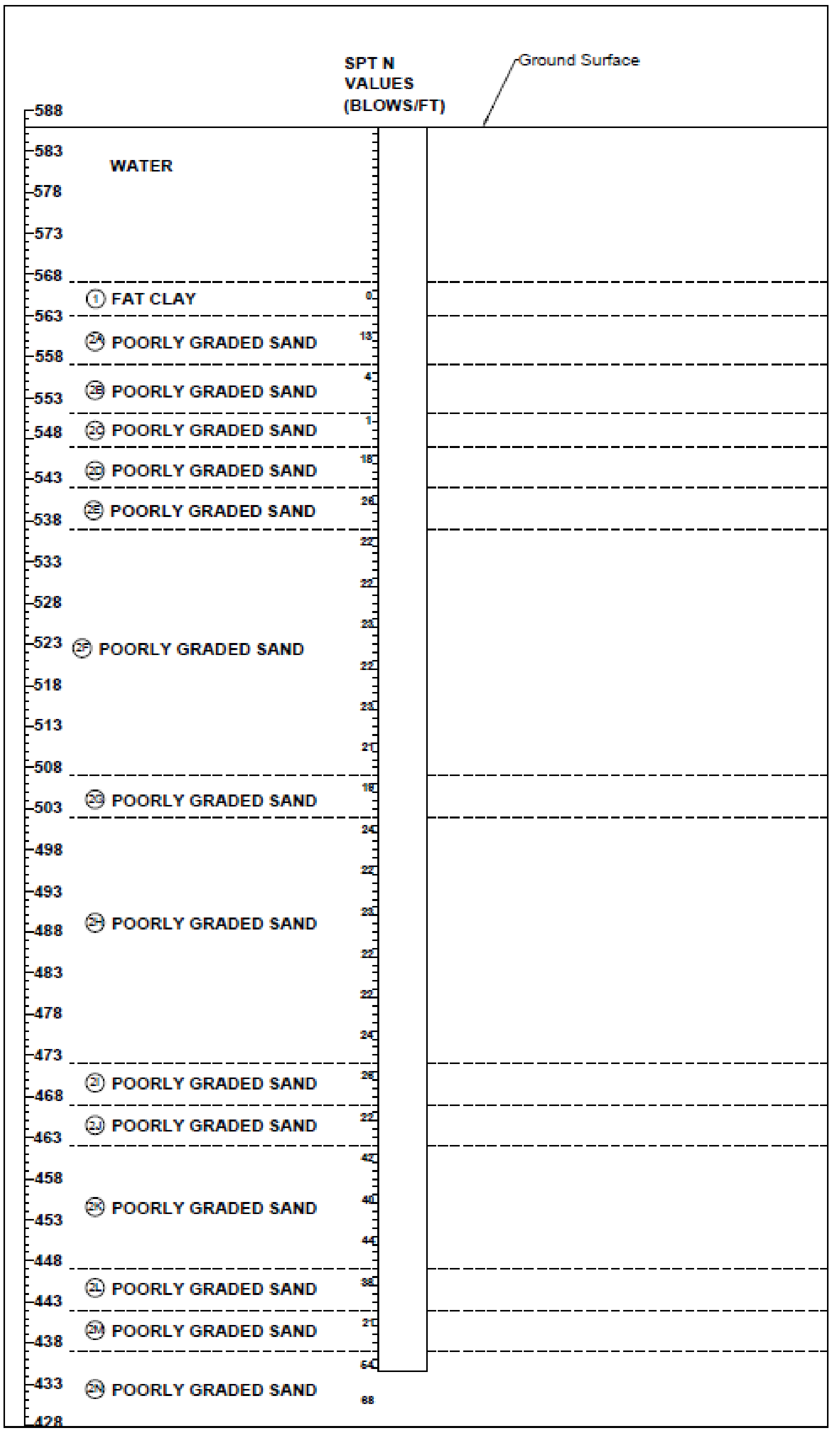

Figure 44. Example 4 soil profile

Step 4. Estimate nominal geotechnical resistance

Based on the soil boring and the recommendations in Chapter 5, the design engineer estimates the nominal unit resistances for friction bearing for each layer, as shown in Table 29 and Table 30.

Table 29. Cohesive soil layers nominal resistance

Soil Layer	Thickness Δh (ft)	SPT N Value	Unit Weight, γ (kcf)	Undrained Shear Strength, S_u (ksf)	α	q_s (ksf)
1	4	0	0.100	0	0	0

Table 30. Cohesionless soil/IGM layers nominal resistance

Soil Layer	Thickness Δh (ft)	SPT N Value	Unit Weight, γ (kcf)	z (ft)	β	σ_v' (ksf)	q_s (ksf)	q_p (ksf)
2A	6	13	0.113	20.5	0.77	0.30	0.23	-
2B	6	4	0.100	26.5	0.25	0.57	0.14	-
2C	4	1	0.078	31.5	0.69	0.71	0.18	-
2D	5	18	0.117	36	0.64	0.88	0.60	-
2E	5	26	0.126	41	0.47	1.17	0.74	-
2F	30	22	0.122	58.5	0.32	2.23	1.04	-
2G	5	19	0.119	76	0.25	3.26	1.05	-
2H	30	23	0.123	93.5	0.25	4.31	1.08	-
2I	5	26	0.126	111	0.25	5.38	1.34	-
2J	5	22	0.122	116	0.25	5.69	1.42	-
2K	15	42	0.128	126	0.25	6.33	1.58	-
2L	5	38	0.122	136	0.25	6.97	1.74	-
2M	5	21	0.121	141	0.25	7.26	1.82	-
2N	5	54	0.140	146	0.25	7.61	1.90	60.00

Step 5. Select resistance factor and estimate factored resistance of each layer

In this step, the design engineer selects the appropriate resistance factor for each soil type. The soil profile in this example is predominantly composed of cohesionless soils and cohesionless IGM. As recommended in Chapter 5, the following resistance factors are used:

φ_{qs} = 0.50 for skin friction in cohesive soil layers
φ_{qs} = 0.75 for skin friction in cohesionless soil layers
φ_{qs} = 0.75 for skin friction in cohesionless IGM layers

Table 31. Factored resistance

Soil Layer	Skin Friction			End Bearing		
	q_s (ksf)	φ_{qs}	R_{sR} (ksf)	q_p (ksf)	φ_{qp}	R_{pR} (ksf)
1	0	0.50	0	-	-	-
2A	0.23	0.75	0.17	-	-	-
2B	0.14	0.75	0.11	-	-	-
2C	0.18	0.75	0.13	-	-	-
2D	0.60	0.75	0.45	-	-	-
2E	0.74	0.75	0.56	-	-	-
2F	1.04	0.75	0.78	-	-	-
2G	1.05	0.75	0.79	-	-	-
2H	1.08	0.75	0.81	-	-	-
2I	1.34	0.75	1.01	-	-	-
2J	1.42	0.75	1.07	-	-	-
2K	1.58	0.75	1.19	-	-	-
2L	1.74	0.75	1.31	-	-	-
2M	1.82	0.75	1.36	-	-	-
2N	1.90	0.75	1.43	60.00	0.50	30.00

Step 6. Estimate contract drilled shaft length, L, based on skin friction

The required shaft length is determined based solely on the factored skin resistance in all soil layers, as determined in Step 5 and presented in Table 31. For this example, a nominal shaft diameter of 6 ft is assumed. The tip resistance is neglected. The cumulative factored geotechnical resistance, R_R, along the shaft is calculated as follows, where L is the total shaft length below the ground surface:

L_0 = 13.2 ft, R_{sR0} = 0
L_1 = 13.2 + 4 = 17.2 ft, $R_{sR1} = R_{sR0}$ + (0 ksf) (4 ft) (π) (6 ft) = 0 kips
L_2 = 17.2 + 6 = 23.2 ft, $R_{sR2} = R_{sR1}$ + (0.17 ksf) (6 ft) (π) (6 ft) = 0 + 18.21 = 19.23 kips
L_3 = 23.2 + 6 = 29.2 ft, $R_{sR3} = R_{sR2}$ + (0.11 ksf) (6 ft) (π) (6 ft) = 19.23 + 12.44 = 31.67 kips
L_4 = 29.2 + 4 = 33.2 ft, $R_{sR4} = R_{sR3}$ + (0.13 ksf) (4 ft) (π) (6 ft) = 31.67 + 9.80 = 41.47 kips
L_5 = 33.2 + 5 = 38.2 ft, $R_{sR5} = R_{sR4}$ + (0.45 ksf) (5 ft) (π) (6 ft) = 41.47 + 42.41 = 83.88 kips
L_6 = 38.2 + 5 = 43.2 ft, $R_{sR6} = R_{sR5}$ + (0.56 ksf) (5 ft) (π) (6 ft) = 83.88 + 52.78 = 136.66 kips
L_7 = 43.2 + 30 = 73.2 ft, $R_{sR7} = R_{sR6}$ + (0.78 ksf) (30 ft) (π) (6 ft) = 136.66 + 441.08 = 577.74 kips
L_8 = 73.2 + 5 = 78.2 ft, $R_{sR8} = R_{sR7}$ + (0.79 ksf) (5 ft) (π) (6 ft) = 577.74+ 74.46 = 652.2 kips
L_9 = 78.2 + 30 = 108.2 ft, $R_{sR9} = R_{sR8}$ + (0.81 ksf) (30 ft) (π) (6 ft) = 652.2 + 458.04 = 1,110.24 kips
L_{10} = 108.2 + 5 = 113.2 ft, $R_{sR10} = R_{sR9}$ + (1.01 ksf) (5 ft) (π) (6 ft) = 1,110.24 + 95.19 = 1,205.43 kips
L_{11} = 113.2 + 5 = 118.2 ft, $R_{sR11} = R_{sR10}$ + (1.07 ksf) (5 ft) (π) (6 ft) = 1,205.43 + 100.85 = 1,306.28 kips
L_{12} = 118.2 + 15 = 133.2 ft, $R_{sR12} = R_{sR11}$ + (1.19 ksf) (15 ft) (π) (6 ft) = 1,306.28 + 336.46 = 1,642.74 kips
L_{13} = 133.2 + 5 = 138.2 ft, $R_{sR13} = R_{sR12}$ + (1.31 ksf) (5 ft) (π) (6 ft) = 1,642.74 + 123.46 = 1,766.2 kips

L_{14} = 138.2 + 5 = 143.2 ft, $R_{sR14} = R_{sR13}$ + (1.36 ksf) (5 ft) (π) (6 ft) = 1,766.2 + 128.18 = 1,894.38 kips
L_{15} = 143.2 + 1.5 = 144.7 ft, $R_{sR15} = R_{sR14}$ + (1.43 ksf) (1.5 ft) (π) (6 ft) = 1,894.38 + 40.43 = 1,934.81 kips

The estimated nominal geotechnical resistance versus depth is presented in Figure 45.

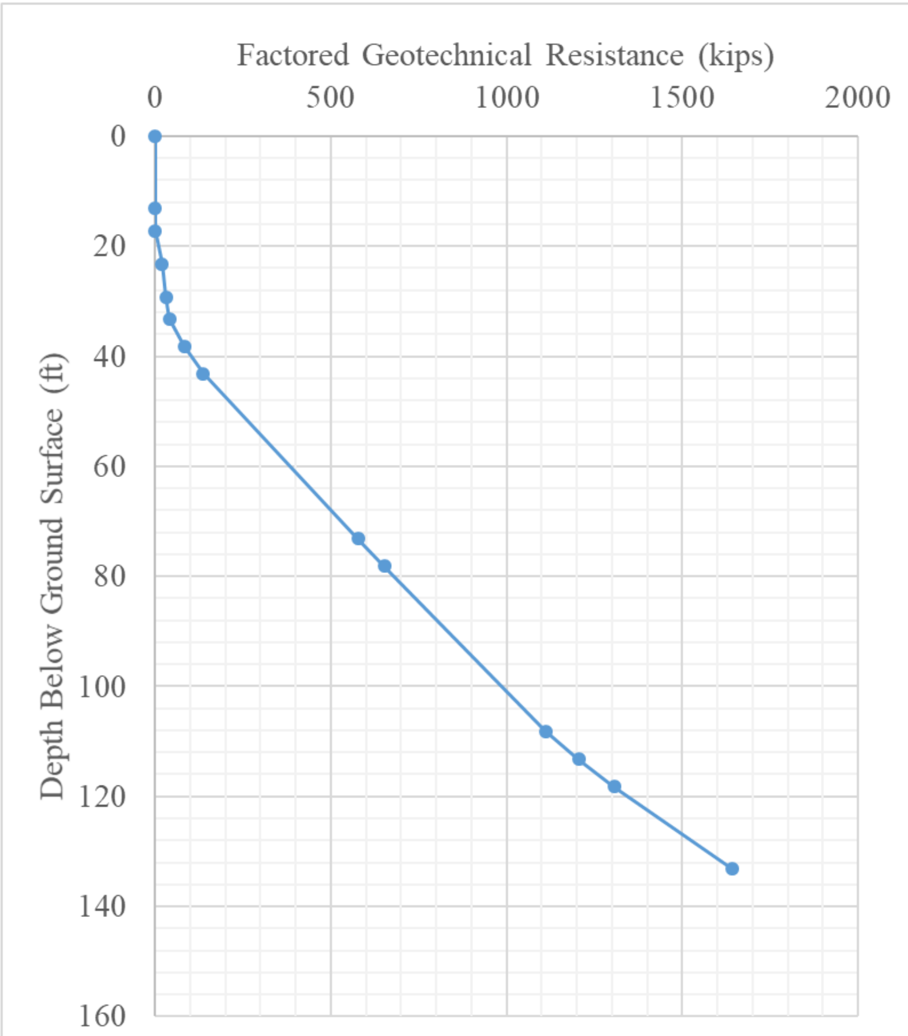

Figure 45. Example 4 plot of nominal geotechnical resistance versus depth

Based on load test data, the measured skin friction at 1 in. top displacement is 2,367 kips, which is above the predicted factored resistance of 1,935 kips. A contract shaft length of 145 ft is adequate to support the required load of 1,500 kips. There is no need to consider resistance from the end bearing. However, doing so could lead to reduced shaft dimensions and reduced project costs.

Step 7. Estimate contract drilled shaft length, L, based on skin friction and end bearing

The required shaft length is determined considering the factored resistance from all sources, including the skin friction and end bearing in all soils. The factored resistances were determined in Step 5 and are presented in Table 31. A smaller nominal shaft diameter of 4 ft is assumed in order to highlight the benefits of including end bearing resistance. The cumulative factored geotechnical resistance, R_R, along the shaft is calculated as follows, where L is the total shaft length below the ground surface:

L_0 = 13.2 ft, R_{sR0} = 0
L_1 = 13.2 + 4 = 17.2 ft, $R_{sR1} = R_{sR0}$ + (0 ksf) (4 ft) (π) (4 ft) = 0 kips
L_2 = 17.2 + 6 = 23.2 ft, $R_{sR2} = R_{sR1}$ + (0.17 ksf) (6 ft) (π) (4 ft) = 0 + 18.21 = 12.82 kips
L_3 = 23.2 + 6 = 29.2 ft, $R_{sR3} = R_{sR2}$ + (0.11 ksf) (6 ft) (π) (4 ft) = 12.82 + 8.29 = 21.11 kips
L_4 = 29.2 + 4 = 33.2 ft, $R_{sR4} = R_{sR3}$ + (0.13 ksf) (4 ft) (π) (4 ft) = 21.11 + 6.53 = 27.64 kips
L_5 = 33.2 + 5 = 38.2 ft, $R_{sR5} = R_{sR4}$ + (0.45 ksf) (5 ft) (π) (4 ft) = 27.64 + 28.27 = 55.91 kips
L_6 = 38.2 + 5 = 43.2 ft, $R_{sR6} = R_{sR5}$ + (0.56 ksf) (5 ft) (π) (4 ft) = 55.91 + 35.19 = 91.1 kips
L_7 = 43.2 + 30 = 73.2 ft, $R_{sR7} = R_{sR6}$ + (0.78 ksf) (30 ft) (π) (4 ft) = 91.1 + 294.05= 385.15 kips
L_8 = 73.2 + 5 = 78.2 ft, $R_{sR8} = R_{sR7}$ + (0.79 ksf) (5 ft) (π) (4 ft) = 385.15 + 49.64 = 434.79 kips
L_9 = 78.2 + 30 = 108.2 ft, $R_{sR9} = R_{sR8}$ + (0.81 ksf) (30 ft) (π) (4 ft) = 434.79 + 305.36 = 740.15 kips
L_{10} = 108.2 + 5 = 113.2 ft, $R_{sR10} = R_{sR9}$ + (1.01 ksf) (5 ft) (π) (4 ft) = 740.15 + 63.46 = 803.61 kips
L_{11} = 113.2 + 5 = 118.2 ft, $R_{sR11} = R_{sR10}$ + (1.07 ksf) (5 ft) (π) (4 ft) = 803.61 + 67.23 = 870.84 kips
L_{12} = 118.2 + 15 = 133.2 ft, $R_{sR12} = R_{sR11}$ + (1.19 ksf) (15 ft) (π) (4 ft) = 870.84 + 224.31 = 1,095.15 kips
L_{13} = 133.2 + 5 = 138.2 ft, $R_{sR13} = R_{sR12}$ + (1.31 ksf) (5 ft) (π) (4 ft) = 1,095.15 + 82.31 = 1,177.46 kips
L_{14} = 138.2 + 5 = 143.2 ft, $R_{sR14} = R_{sR13}$ + (1.36 ksf) (5 ft) (π) (4 ft) = 1,177.46 + 85.45 = 1,262.91 kips
L_{15} = 143.2 + 1.5 = 144.7 ft, $R_{sR15} = R_{sR14}$ + (1.43 ksf) (1.5 ft) (π) (4 ft) + (30.00 ksf) (π) $\frac{(4\text{ ft})^2}{4}$ = 1,262.91 + 26.95 + 376.99 = 1,609.85 kips

The estimated nominal geotechnical resistance versus depth is presented in Figure 46.

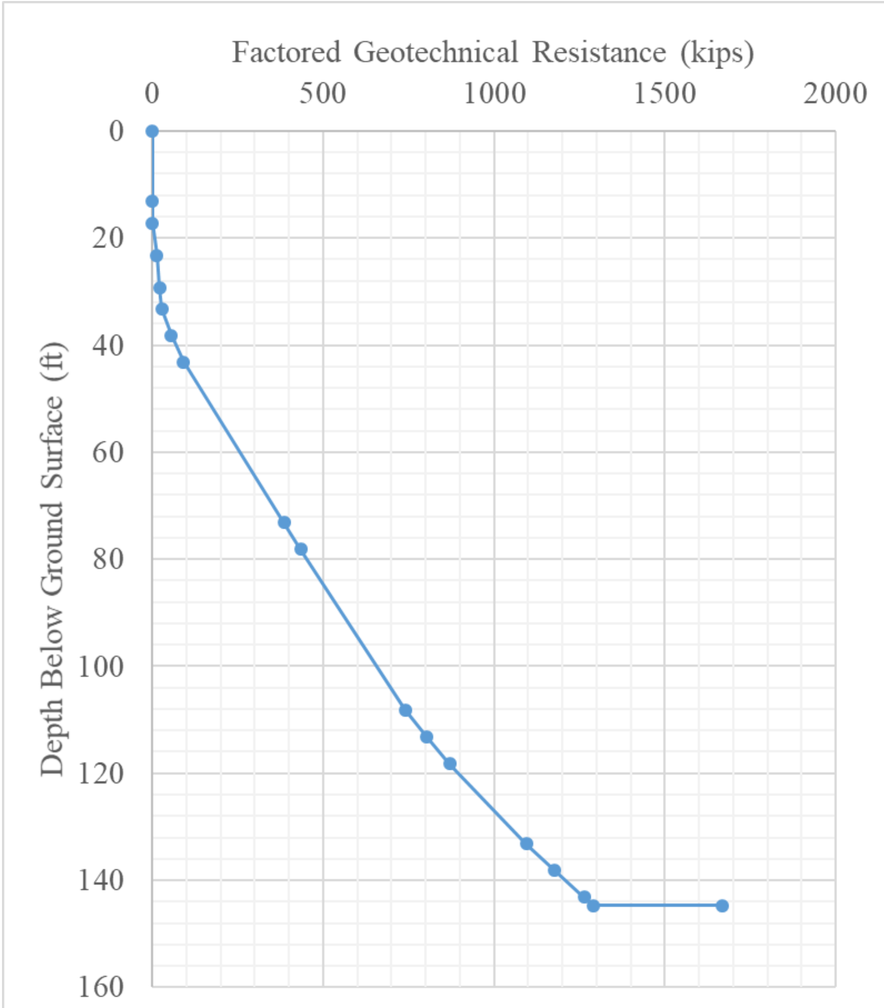

Figure 46. Example 4 plot of nominal geotechnical resistance versus depth

Based on load test data, the measured total load at 1 in. top displacement is 2,210 kips, which is well above the predicted factored resistance of 1,667 kips. If the end bearing and skin friction from the soil layers are considered, the contract shaft length of 145 ft with a smaller diameter of 4 ft can be used to support the anticipated load of 1,500 kips.

Step 8. Check shaft structural capacity

The shaft reinforcement details shall be selected and appropriate checks shall be made to ensure that the design load does not compromise the structural integrity of the shaft.

Step 9. Prepare CADD notes for bridge plans

Step 10. Check the design

THE INSTITUTE FOR TRANSPORTATION IS THE FOCAL POINT FOR TRANSPORTATION AT IOWA STATE UNIVERSITY.

InTrans centers and programs perform transportation research and provide technology transfer services for government agencies and private companies;

InTrans contributes to Iowa State University and the College of Engineering's educational programs for transportation students and provides K–12 outreach; and

InTrans conducts local, regional, and national transportation services and continuing education programs.

INSTITUTE FOR TRANSPORTATION

IOWA STATE UNIVERSITY

Visit **InTrans.iastate.edu** for color pdfs of this and other research reports.